MODELING OF NONLINEAR BEHAVIOR OF STEEL BEAM TO COLUMN SEMI-RIGID CONNECTIONS WITH 3-D SOLID FINITE ELEMENTS

A THESIS SUBMITTED TO
THE GRADUATE SCHOOL OF NATURAL AND APPLIED SCIENCES
OF
MIDDLE EAST TECHNICAL UNIVERSITY

BY

NURETTİN MURAT AZAP

IN PARTIAL FULFILLMENT OF THE REQUIREMENTS
FOR
THE DEGREE OF MASTER OF SCIENCE
IN
CIVIL ENGINEERING

JULY 2013

Approval of the thesis:

MODELING OF NONLINEAR BEHAVIOR OF STEEL BEAM TO COLUMN SEMI-RIGID CONNECTIONS WITH 3-D SOLID FINITE ELEMENTS

Submitted by **NURETTİN MURAT AZAP** in partial fulfillment of the requirements for the degree of **Master of Science in Civil Engineering Department, Middle East Technical University** by,

Prof. Dr. Canan ÖZGEN
Dean, Graduate School of **Natural and Applied Sciences** _____

Prof. Dr. Ahmet Cevdet YALÇINER
Head of Department, **Civil Engineering** _____

Assoc. Prof. Dr. Afşin SARITAŞ
Supervisor, **Civil Engineering Dept., METU** _____

Examining Committee Members

Prof. Dr. Mehmet UTKU
Civil Engineering Dept., METU _____

Assoc. Prof. Dr. Afşin SARITAŞ
Civil Engineering Dept., METU _____

Assoc. Prof. Dr. Oğuzhan HASANÇEBİ
Civil Engineering Dept., METU _____

Asst. Prof. Dr. Ercan GÜRSES
Aerospace Engineering Dept., METU _____

Dr. Cenk TORT
Miteng _____

Date : 11.07.2013

I hereby declare that all information in this document has been obtained and presented in accordance with academic rules and ethical conduct. I also declare that, as required by these rules and conduct, I have fully cited and referenced all material and results that are not original to this work.

Name, Last name : **N. Murat AZAP**

Signature :

ABSTRACT

MODELING OF NONLINEAR BEHAVIOR OF STEEL BEAM TO COLUMN SEMI-RIGID CONNECTIONS WITH 3-D SOLID FINITE ELEMENTS

AZAP, Nurettin Murat

M.S., Department of Civil Engineering

Supervisor: Assoc. Prof. Dr. Afşin SARITAŞ

July 2013, 70 pages

In steel structural systems, beam to column connections are usually assumed either rigid or pinned in practice. In reality rigid connections have some flexibility and shear connections have some rigidity incorporated in their real behavior with significant nonlinearity included, as well; thus this behavior results into the categorization of some connections as semi-rigid. Beam to column connection regions contain one or more of the following components: angles, plates, welds, and bolts. Understanding the physical actions occurring between all these parts is crucial. In this regards the development and use of numerical tools and also further experimental studies trying to identify the monotonic and cyclic behavior of semi-rigid connections have gained significant attention. Detailed modeling and analysis of structural members by using advanced finite element programs is very common nowadays. Conducting experiments may supplement verification of numerical simulations; however experimental works may not be practical in some cases. Despite the advance in computer technology, for the modeling of the complex interaction of geometric and material nonlinearities in steel semi-rigid connections the use of regular computers may not always suffice in terms of computer power and large amounts of analysis time is still needed.

In this thesis 3-D finite element modeling and analysis of semi-rigid connections is undertaken, where for this purpose a special type of bolted beam to column connection is chosen due to its truly semi-rigid characteristic. Previous experiments conducted on this connection type in the last three decades are considered for the numerical study undertaken in this thesis. Results obtained from numerical simulations are compared with experimental data and the reliability of 3-D modeling of connections with the use of advanced nonlinear finite element programs is assessed. In order to model bolted beam to column connections accurately in a numerical simulation for all connection topologies, detailed understanding of the nonlinearities that need to be taken into account during the use of finite element software should be well known. In this

regards, special attention has been given in this thesis for the presentation of how a bolted beam to column connection region shall be modeled, as well.

Keywords: Steel, bolted beam to column connections, semi-rigid connections, finite element method, nonlinear analysis with 3-D finite elements

ÖZ

YARI-RİJİT ÇELİK KİRİŞ-KOLON BAĞLANTILARIN DOĞRUSAL OLMAYAN DAVRANIŞININ 3 BOYUTLU SONLU ELEMANLARLA MODELLENMESİ

AZAP, Nurettin Murat

Yüksek Lisans, İnşaat Mühendisliği Bölümü

Tez Yöneticisi: Doç. Dr. Afşin SARITAŞ

Temmuz 2013, 70 sayfa

Pratikte, çelik yapı sistemlerindeki kiriş–kolon bağlantıları genellikle ya rijit (moment) ya da basit (mafsal) bağlantı tipleri olarak varsayılmaktadırlar. Gerçek durumda bağlantı tiplerinin dikkate değer lineer olmayan davranışları göz önüne alındığında, rijit bağlantıların bir miktar esnekliğe sahip olduğu ve basit bağlantıların da bir miktar rijitliğe sahip oldukları, hatta bu sebepten dolayı da bazı bağlantı tiplerinin yarı-rijit bağlantı adı altında kategorize edildikleri bilinmektedir. Kiriş-kolon bağlantı bölgeleri bir ya da birden fazla sayıda/miktarda köşebent, plaka, kaynak ve bulon gibi birleşenleri içermektedirler. Tüm bu bileşenlerin birbirleri ile olan fiziksel etkileşimlerinin anlaşılması son derece önemlidir. Bu bakımdan, sayısal programlar kullanarak ve deneysel çalışmalar yürüterek yarı-rijit bağlantıların monotonik ve çevrimsel davranışlarının araştırılması çok önemli bir ilgi konusu haline gelmiştir. Yapısal elemanların detaylı analizi ve modellenmesi için gelişmiş sonlu elemanlar programlarının kullanımı çok yaygın hale gelmiştir. Sayısal simülasyonların deneyler ile tamamlanması mümkündür ancak, deneysel çalışmaların yürütülmesi bazı durumlarda pratik olmayabilmektedir. Bilgisayar teknolojisindeki ilerlemelere rağmen, yarı-rijit bağlantılardaki doğrusal olmayan geometrik ve malzeme davranışlarının karmaşık özelliğinin modellenmesi günlük bilgisayar kullanımı ile yetersiz kalabilmekte ve uzun zamanlar alabilmektedir.

Bu tezde yarı-rijit bağlantıların üç boyutlu sonlu elemanlarla modellenmesi ve analizi gerçekleştirilmiş ve karşılaştırmalar özellikle bulonlu kolon-kiriş bağlantıların yarı-rijit karakteristiğine odaklanmıştır. Yapılan araştırmalar sonucu bulunmuş, son 30 yılda bu bağlantı tipi ile ilgili gerçekleştirilmiş deneysel çalışmalar bu tez kapsamı altında dikkate alınmıştır. Sayısal simülasyonların sonuçları, deneysel veriler ile karşılaştırılmış ve gelişmiş lineer olmayan sonlu elemanlar programı ile modellenmiş üç boyutlu bağlantı modellerinin güvenirliliği bulunmaya çalışılmıştır. Bulonlu kolon-kiriş tipi bağlantıların doğru olarak sayısal bir biçimde modellenebilmeleri için, sonlu elemanlar programlarının kullanımlarının ve lineer olmayan

davranışların detaylı bir biçimde bilinmeleri gerekmektedir. Bu bakımdan bulonlu bir kolon-kiriş bağlantısının modellenmesi ile ilgili özel bir sunum da bu tez kapsamında verilmiştir.

Anahtar Kelimeler: Çelik, bulonlu kiriş-kolon bağlantıları, yarı-rijit bağlantılar, sonlu elemanlar yöntemi, üç boyutlu sonlu elemanlarla doğrusal olmayan analiz

ACKNOWLEDGMENTS

I wish to express my deepest gratitude to my supervisor and mentor Assoc. Dr. Afşin SARITAŞ for his continuous support, guidance, advice, criticism, encouragements and insight throughout the thesis work and also during my graduate student life.

The help, tolerance, patience and continuous support of my friends, colleagues and all previous & current business managers are also acknowledged with great appreciation.

I wish to express my sincere thanks to the professors and faculty members for advice and valuable knowledge that I got from them during my graduate education. In this regards, I would like to say thanks especially to Assoc. Prof. Ayşegül ASKAN GÜNDOĞAN for being both a friend & a professor in this period.

I would especially like to express my deepest thanks to my second sister Yaşam KIZILDAĞ, who has always been with me from high school to the end of graduate life with endless support, patience and friendship.

I am most grateful for being one of the most patient and supportive person in my graduate student life for Duygu Melis ARSLAN. She has always supported and encouraged me from the beginning to the end of my study & graduate life with boundless patience and compassion. In this regards, I would specially like to thank her.

This thesis is especially dedicated to my family members and I would also like to offer my deepest thanks to each of my family members; my mother S. Gülşen AZAP, my father Selçuk AZAP, my sister Tuğba ÇAYIRCIOĞLU & my brother Z. Cenk ÇAYIRCIOĞLU for their patience, infinite support and endless love during my study & life. Also I would like to thank my nephew Zeynep ÇAYIRCIOĞLU for being my source of happiness.

TABLE OF CONTENTS

LIST OF TABLES

TABLES

LIST OF FIGURES

FIGURES

LIST OF SYMBOLS AND ABBREVIATIONS

3-D	Three Dimensional
θ_R	Rotation
AISC	American Institute of Steel Construction
ASTM	American Society for Testing and Materials
DWA	Double Web Angle
FE	Finite Element
M	Moment
SWAP	Single Web – Angle / Plate
TSA	Top and Seat Angle
TSADWA	Top, Seat and Double Web Angle

CHAPTER 1

INTRODUCTION

1.1 General

Members forming steel structural systems such as beams, columns, bracings, flooring and roofing systems are all separately fabricated and connected to each other during construction. The relative motion of the connecting parts could be simply idealized as either fully restrained or partly free to move. Among all these connections, beam to column connections are usually considered as the most important part of a steel structure. Beam to column connections are usually assumed either rigid (fully restrained against rotation) or pinned (free to rotate) in practice (Citipitioglu et al. 2002). These two end cases are idealizations of reality and there is always partial restraint provided by the connection region. For some connection types though the behavior of the connection is much different than these two ideal end cases and these types of connections are called as partially restrained or semi-rigid. Beam to column connection regions contain one or more of the following components: angles, plates, welds, and bolts. There is some flexibility/rigidity provided by the connection region due to the presence of all these parts when compared with respect to the ideal two end cases. Especially after Northridge Earthquake in 1994 and Kobe Earthquake in 1995, nonlinear behavior of a connection became a critical issue for the performance assessment of a structure during severe ground motions. In this regards the development and use of numerical tools and also further experimental studies trying to identify the monotonic and cyclic behavior of semi-rigid connections have gained significant attention.

Detailed modeling and analysis of structural members by using advanced finite element programs is very common nowadays, especially if the real behavior of that member is a matter of interest for the designer or researcher. Conducting experiments may supplement numerical simulations in some cases; however experimental works may not be feasible and possible in some commercial projects or scientific studies. Researchers in academic institutes often use numerical simulations in order to assess the validity of available nonlinear analysis modules provided by software packages. With the advance in computer technology, regular computers are easily used towards that aim and results can be obtained in a relatively short amount of time in most cases. With respect to the modeling of the complex interaction of geometric and material nonlinearities in steel semi-rigid connections, the use of regular computers may not always suffice in terms of computer power, and large amounts of analysis time is still needed.

This thesis will focus on top and seat with double web angles (TSADWA) connection due to its rising use in practice and also rising interest in research community due

to its truly semi-rigid characteristics in terms of initial stiffness, strength and ductility. The first experiment conducted towards understanding the nonlinear behavior of this connection was undertaken by Rathbun (1936). 50 years after that study, Azizinamini (1985) conducted experiments on TSADWA connection and published his work. In the last decade and a half, two further experimental studies were conducted on this connection type (detailed literature review is given later in this chapter). With respect to the numerical simulation and validation of finite element modeling capabilities, researchers only considered the tests conducted by Azizinamini up to now for TSADWA connection type. This thesis will encompass all TSADWA connection tests conducted in the last three decades, the results obtained from numerical simulations will be compared with experimental data and the reliability of 3-D modeling of connections with the use of advanced nonlinear finite element programs will be assessed. In order to model bolted beam to column connections accurately in a numerical simulation for all connection topologies, detailed understanding of the nonlinearities that need to be taken into account during the use of finite element software package should be well known. In this regards, special attention has been given in this thesis for the presentation of how a bolted beam to column connection region is modeled in ANSYS Workbench, as well.

In the next section, detailed review on the types of semi-rigid steel connections, literature review on TSADWA semi-rigid connection tests and the numerical simulations undertaken by the use of 3-D finite element programs will be provided in detail.

1.2 Semi-Rigid Connection Types

Steel is one of the most preferred, studied and known structural material in construction sector, yet there are still some uncertainties with regards to the behavior of some of its parts especially under high seismicity, such as the nonlinear behavior of the connection regions.

Significant amount of research has been carried and are still going on in order to understand the physical actions and resulting responses occurring in various types of steel connections. As mentioned before, there is an assumption related with the behavior of steel connections in practice, i.e. the fully rigid or ideally pinned cases. A wrong designed connection can cause catastrophic failures for the whole structural system due to wrong assumptions/ design calculations or incorrect implementations on the construction site. In order to prevent these undesired situations, all assumptions and design variables should be selected correctly. In other words, all related researches and structural codes should be well known. Various steel connections used nowadays actually deviate from the fully rigid case both in terms of stiffness and strength. Furthermore, deformation demands imposed on these types of connections are off special interest and the assumption of fully rigid connection type for these pose significant potential problems.

In order to analyze semi-rigid connection behavior accurately, the moment rotation curves provide the means of realizing the capacity provided by the connection and the

production of these curves have the utmost importance. For instance, top and seat angles and double web angles (TSADWA) connection type have higher moment capacity when compared with the double web angles (DWA) connection. As a general rule of thumb, a stiffer connection usually has higher moment capacity. Typical moment-rotation curves for various semi-rigid connection types have been presented in Figure 1.1.

In the following, all semi-rigid connection types used popularly in practice will be presented.

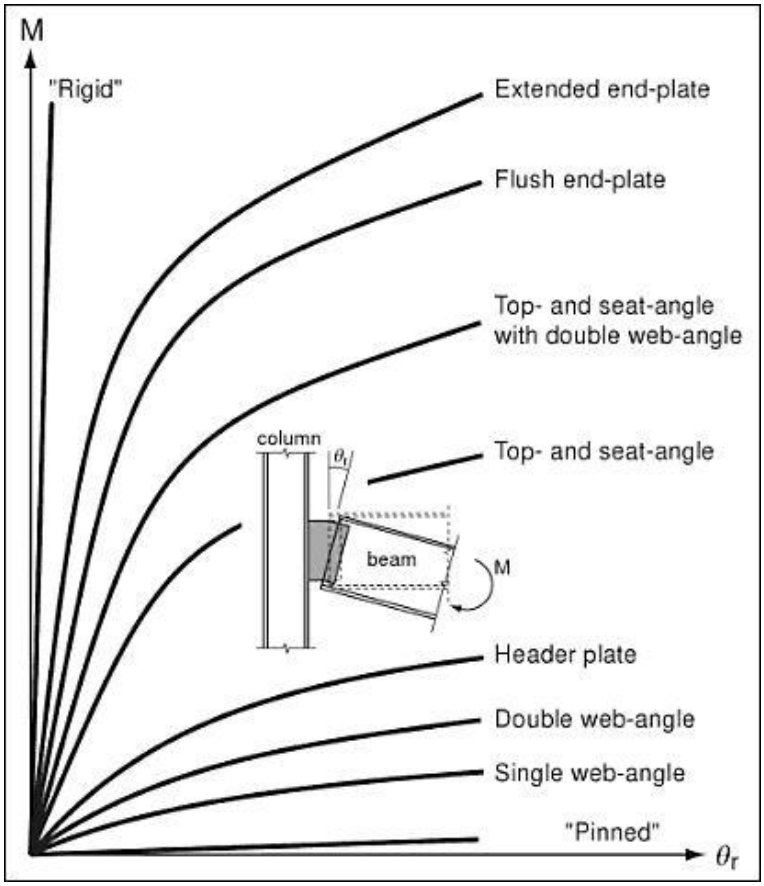

Figure 1.1 Typical Moment – Rotation (M - θ_R) Curve for Beam – Column Connection Azizinamini (1985)

1.2.1 Single Web – Angle / Plate Connections

In single web angle/plate (SWAP) type of connections, column and beam profiles are connected to each other with the help of a simple angle or plate. The single web angle (L profile) connection type can be seen in Figure 1.2 and also the single web plate connection type can be found in Figure 1.3.

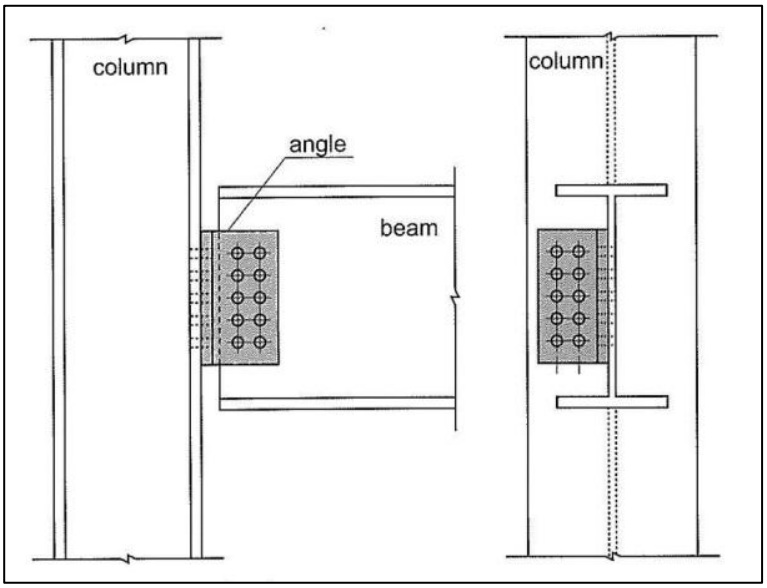

Figure 1.2 Single Web Angle (L Profile) Connection Type, Chen et al. (2011)

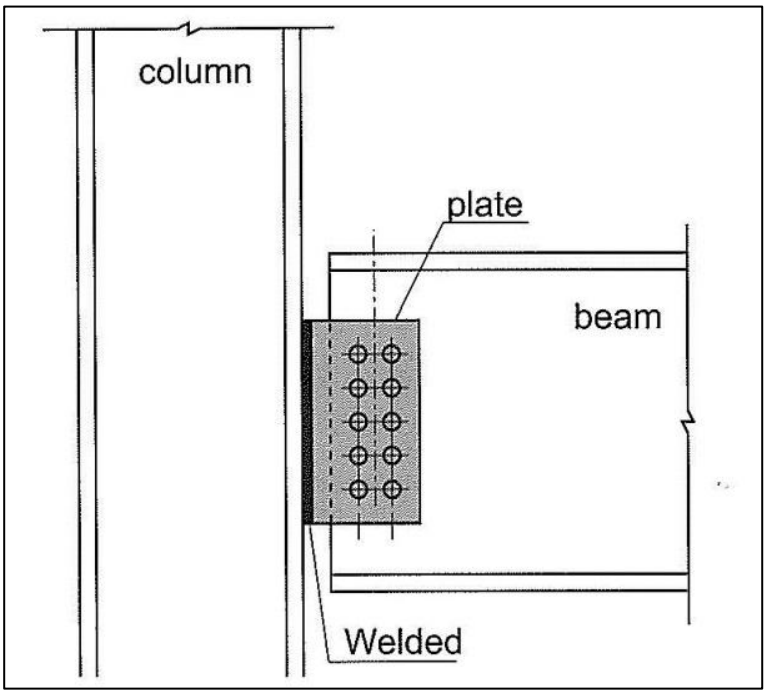

Figure 1.3 Single Web Plate Connection Type, Chen et al. (2011)

The single web angle (L profile) connection type has bolts that connect the beam and column to the angle body only from one side of the beam. With the help of these bolts' shear and tensile force capacities, the designer can connect the beam and column to each other. It can be easily observed that the single web angle connection has half the moment capacity of double web angle connections.

The single web plate connection has a welded connection type supported with bolts as shown in Figure 1.3. The beam or column section is welded to the plate and the opposite of welded section has the mechanical bolted connection. This kind of connection helps the worker in terms of construction ease.

As part of this connection type, when these sub-types are compared with each other, rigidity of the single plate type of SWAP connection is equal or greater than the single web angle connections.

1.2.2 Double Web – Angle Connections

Double web angle (DWA) type of connection has two angles (L profiles) connecting the column and beam profiles by the help of bolts as shown in Figure 1.4.

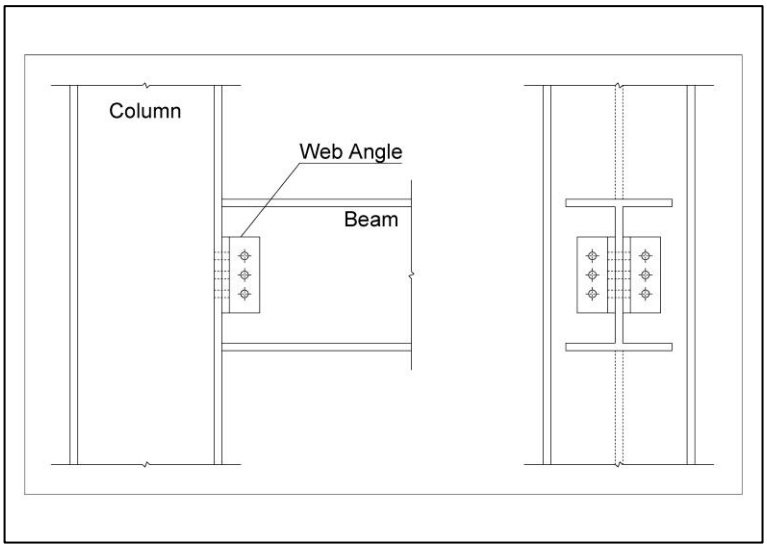

Figure 1.4 Double Web Angles Connection Type

In DWA connection, the column and beam profiles connect with each other with usually two identical and opposite sided L angles with the help of bolts. Previously, rivets were used in order to connect these profiles with each other instead of bolts. Improvements in the production of high strength bolts lead to their widespread use, and most of the specifications allow the use of bolts instead of rivets. According to AISC-ASD specifications (1989), double web angle type of connection is considered as simple (shear) connection.

1.2.3 Top and Bottom L Angle Connections

Top and seat angles (TSA) connection type has two angles (L profiles) that connect the column and the beam by the help of bolts to each other as shown in Figure 1.5.

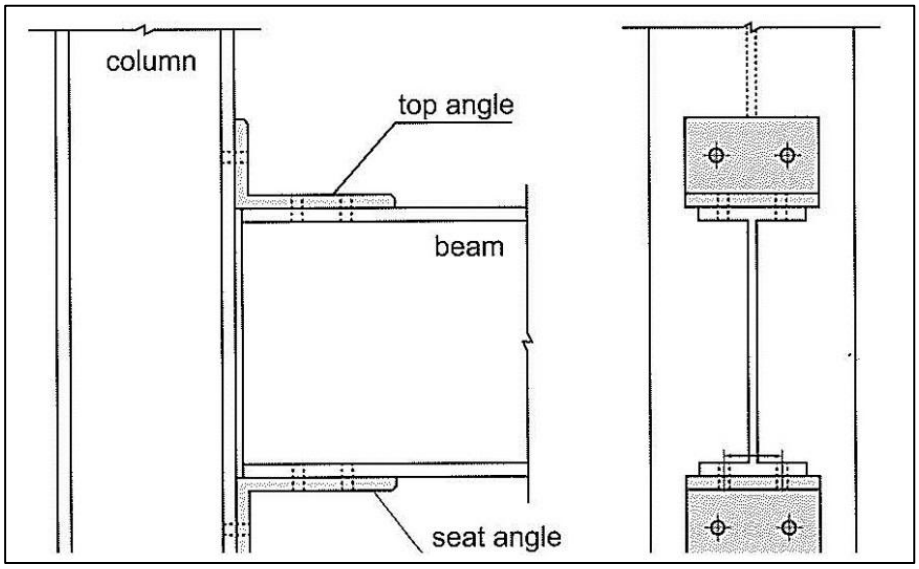

Figure 1.5 Top and Seat Angles Connection Type, Chen et al. (2011)

According to AISC-ASD specifications (1989), the top angle provides lateral support of the compression flange of the beam, on the other hand the bottom or also called as seat angle is for transferring only the vertical reaction from the beam to column (not transfers any moment to the end of the beam). Obviously under cyclic loading conditions these assumptions can be generalized for positive and negative cycles of loading conditions. Experimental results show that these kinds of connections are able to transfer some moment forces between the beam and the column.

1.2.4 Top and Seat Angles with Double Web Angles Connections

Top and seat angles with double web angles (TSADWA) connection type has four angles (L profiles) that connect the column and the beam by the help of bolts to each other as shown in Figure 1.6.

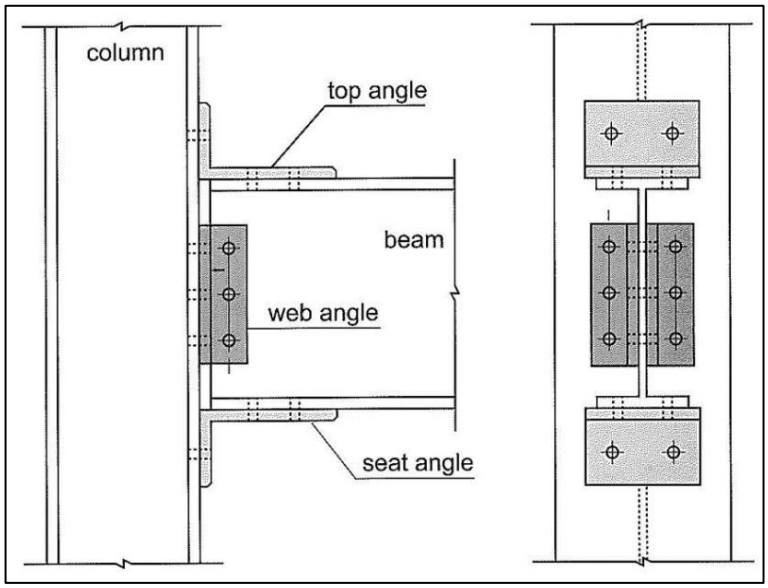

Figure 1.6 Top and Seat Angles with Double Web Angles Connection Type Chen et al. (2011)

In order to transfer the shear forces and to improve connection restraint, double web angles are added to top and seat angles type of connection. According to AISC-ASD specifications (1989), this type of connection is considered as "semi-rigid".

1.2.5 Plate Welded Connections

Plate welded connections have only a plate connecting the column and the beam by the help of bolts and welds to each other. There are several different types of plate welded connections;

- Extended end-plate (only tension side) (Figure 1.7)
- Extended end-plate (both tension and compression side) (Figure 1.8)
- Flush end-plate (Figure 1.9)
- Header plate (Figure 1.10)

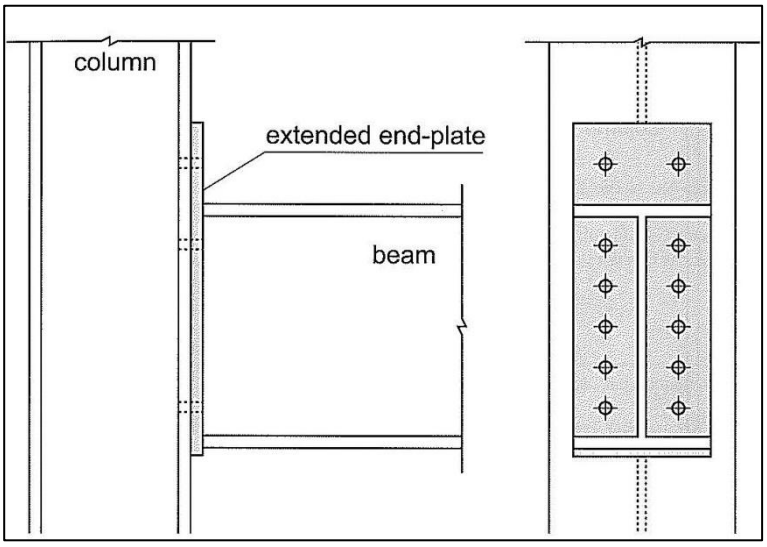

Figure 1.7 Extended End-Plate (Only Tension Side) Connection Type
Chen et al. (2011)

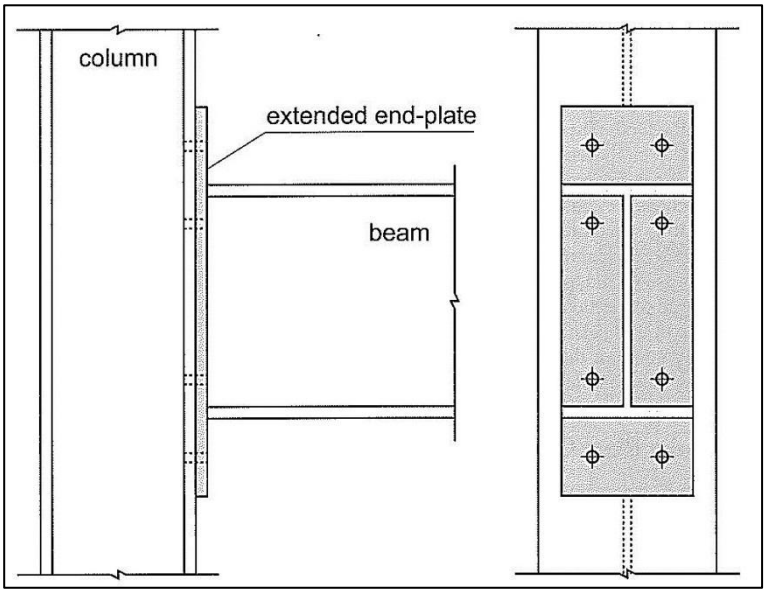

Figure 1.8 Extended End-Plate (Both Tension and Compression Side) Connection Type
Chen et al. (2011)

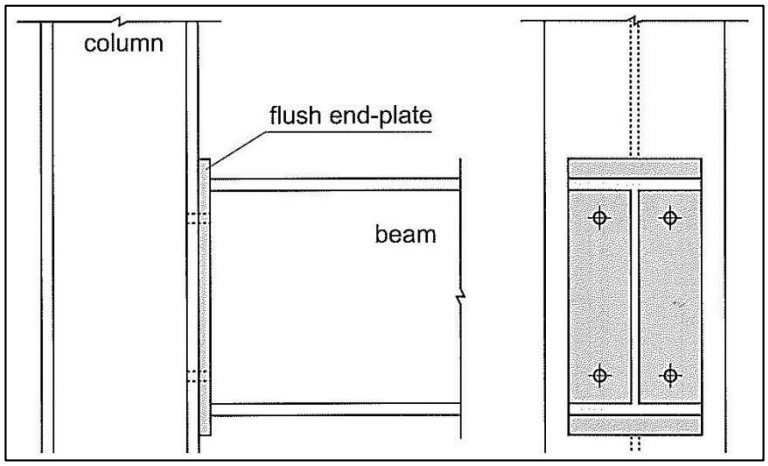

Figure 1.9 Flush End-Plate Connection Type, Chen et al. (2011)

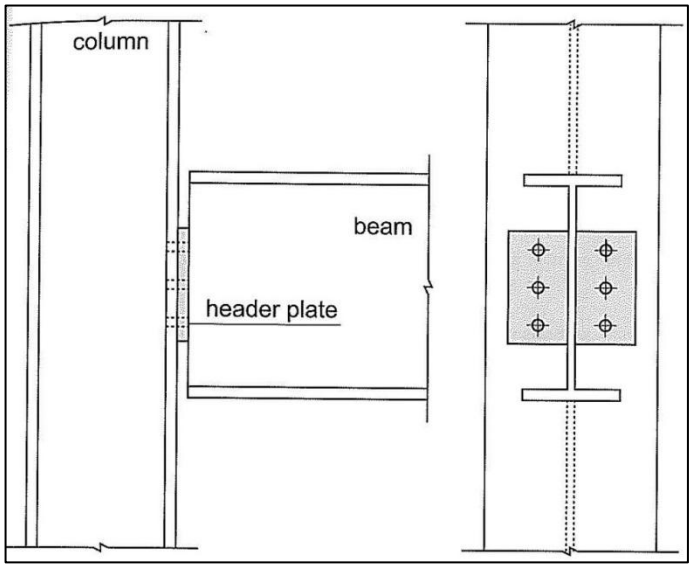

Figure 1.10 Header Plate Connection Type, Chen et al. (2011)

Practically, engineers usually design the structures as welded to the beam (on production process) and bolted to the column (on site) in order to attain the ease of assembly for the workers. As known, the shear and tensile strength values of welds are not greater than the steel's strength values and also welding process should be done in clean surface conditions. Welder's capability and site conditions can prevent the production of strong and clean weld connections between the column and the beam.

1.3 Literature Review

This section presents the research studies on the experimental works and 3D nonlinear finite element modeling and simulations on top and seat angles with double web angles (TSADWA) connections. First the experimental research studies will be presented, and then the numerical studies will be given.

1.3.1 Experimental Studies

Initial experimental studies related with semi-rigid connections were conducted with rivets instead of bolts prior to 1950s. Rathbun (1936) was the first researcher conducting experiments on TSADWA connections, and he used rivets on the column and beams in order to connect them to each other. Rathbun carried out 7 DWA connection tests, 3 TSA connection tests, and 2 TSADWA connection tests.

With the use of high strength bolts, rivets are interchanged with bolts almost in most experimental studies conducted on beam to column connections.

The main experimental work conducted on TSADWA connections was carried at University of South Carolina by Azizinamini (1985). In his Ph.D. study, Azizinamini conducted 20 TSADWA connection tests and 2 TSA connection tests, where the material properties related to the steel profiles were all documented; however no information related to bolts were given. Azizinamini investigated mostly monotonic loadings on the connections, but cyclic loading effects were also considered in some specimens. Azizinamini provided experimental results in terms of moment-rotation curves, and all of those curves had smooth polynomial shape.

Calado et al. (2000) conducted 15 TSADWA connections tests in which 3 different sizes of top, bottom and web angles were considered. The main purpose of the experimental study was to improve the experimental database on TSADWA connections for both monotonic and cyclic loading conditions. The comparison between the monotonic and cyclic loading tests revealed minimal effect on strength and stiffness degradation due to loading reversals. Furthermore, the cyclic moment-rotation curves of that study clearly showed significant pinching effects.

Komuro et al. (2003) conducted 1 TSA and 2 TSADWA connection tests under both monotonic and cyclic loading conditions. The experimental moment rotation curves obtained from the study were compared with the equations suggested by Kishi and Chen (1990) for TSDWA connections under monotonic loading conditions, and good match was attained. One of the important conclusions of that study was the significance of pinching effect in the definition of cyclic moment-rotation behavior.

It is evident that the amount of experimental work undertaken on TSADWA connections is few, especially when compared with other connection types. Detailed

documentation of experimental studies on all connection types listed in Section 1.2 could be found in Chen et al. (2011).

1.3.2 Numerical Simulations

In this section, research studies focusing on 3-D detailed modeling of the connection region with bolts, contact, friction and pretension besides all the material and geometrical nonlinearities will be documented.

Initial attempts to model steel connections were undertaken without the use of available finite element software such as ANSYS or ABAQUS. In the study by Krishnamurthy and Graddy (1976) and in a later study by Krishnamurty (1980), finite element method was employed for the modeling of bolted steel connections, where linear elastic material conditions and the use of eight node elements were considered. Contact was artificially provided through attaching and releasing nodes on the presence of compressive or tensile normal stress distributions on the contact surfaces, respectively.

With the rise of advanced software packages especially by the end of 1990's, numerical simulations tried to bring in as many nonlinear actions as possible. Yang et al. (2000) modeled double web angles connections with angles bolted to column and welded to beam, where ABAQUS finite element program was used in order to get the moment- rotation curves under elastic-perfectly plastic material behavior. In their analysis, contact between the bolt heads and the angles was considered, but contact and bearing interaction between the bolt shanks and bolt holes was neglected.

Citipitioglu et al. (2002) carried out one of the most elaborate numerical study on TSADWA connections, in which ABAQUS finite element program was used and the monotonic experiments conducted by Azizinamini were considered only. In their study, they used all capabilities provided by ABAQUS and considered contact and friction effect between surfaces. Since Azizinamini (1985) did not provide information on bolt material properties and bolt pretension values, Citipitioglu et al. (2002) worked on a calibration method for the determination of these. It was concluded that the bolt pretension value is important in terms of closely matching the numerical results with experimental ones. In terms of bolt material properties, nominal values were used.

Danesh et al. (2006) also considered the monotonic experiments carried out by Azizinami, and used ANSYS finite element program to get moment-rotation type curves for TSADWA connections. In their study, they compared the numerical results from their study with the experimental data and also with the numerical results of Citipitioglu et al. (2002). The calibration of material properties was similar to the effort by Citipitioglu. Bolt pretension was applied as first load case in analysis, and then transverse displacement was imposed on the beam.

In a later study by Uslu and Saritas (2010), monotonic experiments carried out by Azizinamini were used for 3-D finite element modeling of TSADWA connections, and the reliability of proposed simplified mathematical models in literature were assessed.

Within the scope of this thesis, previous experimental studies undertaken on TSADWA connections in the last 3 decades will be considered for numerical modeling, and the validity of using current software packages in estimating the main nonlinear phenomena in TSADWA connections will be assessed, in terms of estimation of initial stiffness, hardening slope and plastic moment capacity.

1.4 Organization of Thesis

This thesis is divided into four chapters. The first chapter begins general introduction and continues with information regarding to the steel connection types, and ends with literature review on experimental and numerical studies on top and seat angles with double web angles connections.

The second chapter presents the use of ANSYS Workbench finite element program towards detailed modeling of beam to column connection region with bolts, pretension, contacts, friction and material and geometric nonlinearities. First, the type of material models that can be used in ANSYS is given, and then meshing procedures and modeling of bodies and bolts are explained in great length. The time consumption records are given and the contact properties and bolt pretension definitions that need to be employed in analysis are clarified with demonstrations.

In the third chapter, experimental studies from previous experimental research studies conducted on top and seat angles with double web angles connection were compared with the finite element model results obtained from current work. Information about the experimental studies is also given.

The last chapter contains the summary and conclusion sections. In order to lead the future researchers related with the semi-rigid finite element modeling, suggestions and recommendations are provided.

CHAPTER 2

FINITE ELEMENT MODELING OF NONLINEAR SEMI-RIGID CONNECTIONS

This chapter presents the nonlinear finite element modeling of semi-rigid connections by using ANSYS Workbench. Modeling a detailed response of steel beam to column connection region resulting from the complex interaction of material, geometric and contact nonlinearities in ANSYS is still a fairly difficult effort to undertake. Commercial programs nowadays have vast element and material libraries for the solution of nonlinear material and geometric problems in structural mechanics. In this regards, ANSYS provides all of these modeling and solution strategies and is actually one of the most popular and advanced finite element program related with engineering design and analysis. With technological improvements in the last two decades, users of finite element programs demand friendlier user interfaces in order to define complex physical problems in ANSYS. This demand pushed the developers of ANSYS to provide the Workbench module and improve its capabilities. Despite the fact that Workbench module of ANSYS provides simplifications to the users with respect to its classical version, users still face with significant modeling difficulties especially in structural mechanics problems.

In this chapter, defining and meshing the geometrical shapes with all its bodies, contact between surfaces, pretension in the bolts, definition of nonlinear material parameters and eventually the solution strategies through the use of ANSYS Workbench will be presented. Furthermore, small scale examples will demonstrate the relevance of the effort presented in this chapter with the research study conducted in the later chapters.

2.1 Material Properties & Models

Engineering Data module of ANSYS Workbench provides the following 3-D nonlinear constitutive models for the definition of 3-D stress-strain relations for steel material.

- Bilinear isotropic hardening
- Multilinear isotropic hardening
- Bilinear kinematic hardening
- Multilinear kinematic hardening

Nonlinear material parameters that need to be provided in *Engineering Data* module base on uniaxial tests. It is well known that hardening in steel is mostly associated with kinematic hardening; thus isotropic hardening in steel could be assumed zero except than

low-cycle and high-cycle fatigue analyses. In this thesis, bilinear kinematic hardening model without any isotropic hardening is used.

2.2 Meshing

The meshing procedure is one of the most important parts of the modeling of the physical domain in any finite element analysis. As the name itself implies, a continuous body is actually meshed through a finite number of elements. The accuracy of the meshed domain could be assessed through further refinement of the body parts and comparison of the results between three different levels of mesh refinement. It is also important to identify the regions where strong nonlinearities would be present, and such regions should actually be treated separately and meshed finer as a subdomain. A very fine mesh usually results in extremely long analysis durations and the creation of large amount of data. Thus, the selection of a medium fine mesh would both provide sufficiently accurate results and reliable solution to the users. In this section of the chapter, the preferred meshing strategy is presented in detail next.

There are 8 main types of the meshing options for the users in ANSYS Workbench *Static Structural* module (see Figure 2.1):

1) Method,
2) Sizing,
3) Contact Sizing,
4) Refinement,
5) Mapped Face Meshing,
6) Match Control,
7) Pinch,
8) Inflation

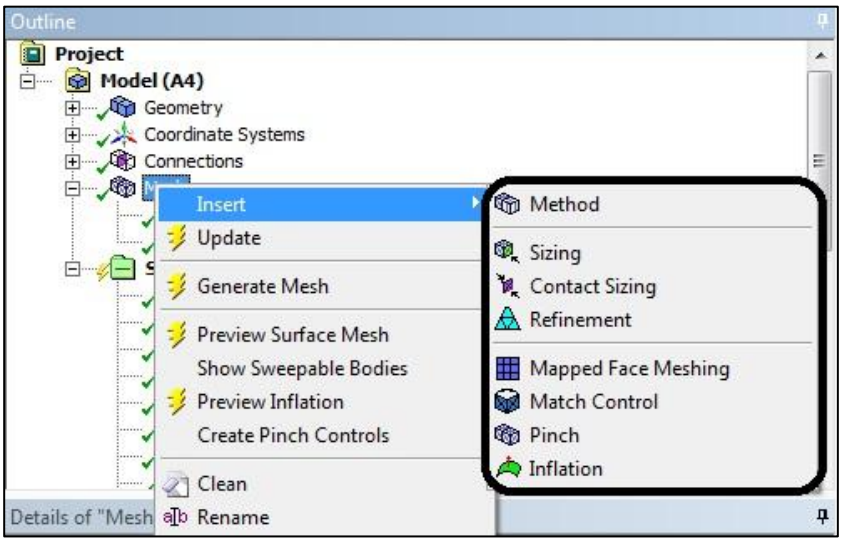

Figure 2.1 Meshing Type Options, ANSYS Workbench

After the user completes drawing the geometry of the physical body, ANSYS Workbench provides automatic or selective meshing of the domain. The sizing of the mesh could be set with “sizing” option in various ways. One of the options for setting the meshing is relevant center module. The user could select from 3 options that are “coarse / medium / fine”. These options are the automatic meshing sizing provided by ANSYS, where the default mode is “coarse”. The alternative for sizing of the mesh is manual selection of element size as shown in Figure 2.2.

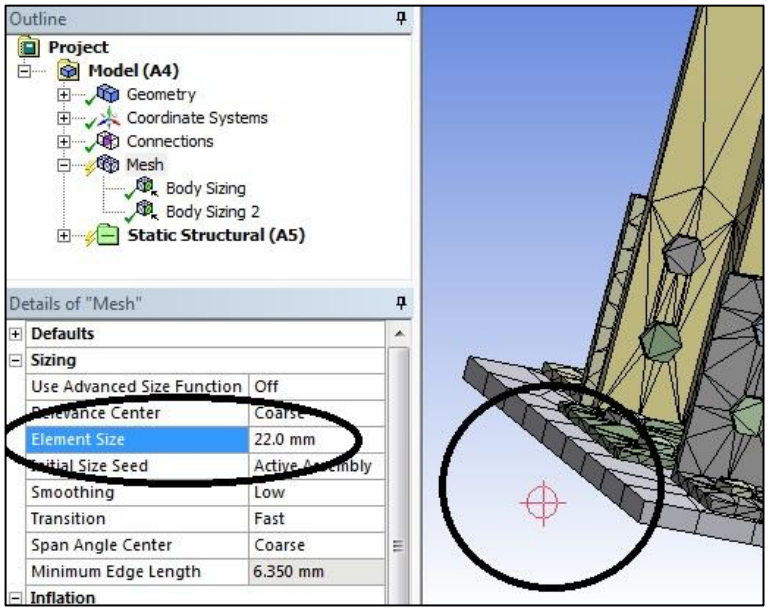

Figure 2.2 Element Size of the Mesh, ANSYS Workbench

The type of solid finite element that will be used in the analysis can be selected through an indirect input of whether element midside nodes will be kept or dropped. An 8-node brick element does not have any midside nodes and results into linear shape functions for the approximation of element displacement field, while the use of midside nodes results in higher order shape functions. The solid element’s midside nodes could be defined through “Element Midside Nodes” option in ANSYS Workbench as shown in Figure 2.3. In this thesis, midside nodes option is selected as “program controlled”.

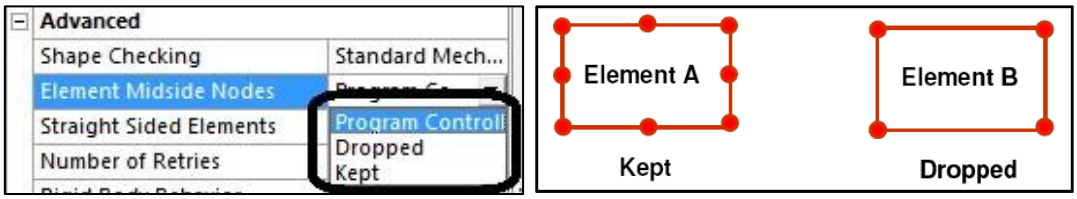

Figure 2.3 Element Midside Nodes, ANSYS Workbench

In order to get more accurate nonlinear behavior and save in solution time, only connection region is meshed finer in this thesis. In the next subsections, meshing of the various parts of the physical domain is discussed.

2.2.1 Meshing for Bolts

Different meshing strategies could be employed on different bodies of a bolted semi-rigid steel connection. The bolt shank, nuts and the contact surfaces between the bolts and the steel beam and column are the most important regions in terms of meshing. In Figure 2.4, different meshing strategies are presented and discussed below:

- The right top bolt has the same mesh sizing of 5 mm for the bolt shank and nuts.
- The left top bolt is an example for a finer meshing along bolt shank. If the designer tries to investigate the stress distributions more accurately on bolt shank, this kind of meshing could be employed.
- The right bottom bolt has much finer mesh sizing compared to the left top bolt.
- Left bottom bolt shows the automatically generated mesh with user selection of "refinement" option in ANSYS Workbench.

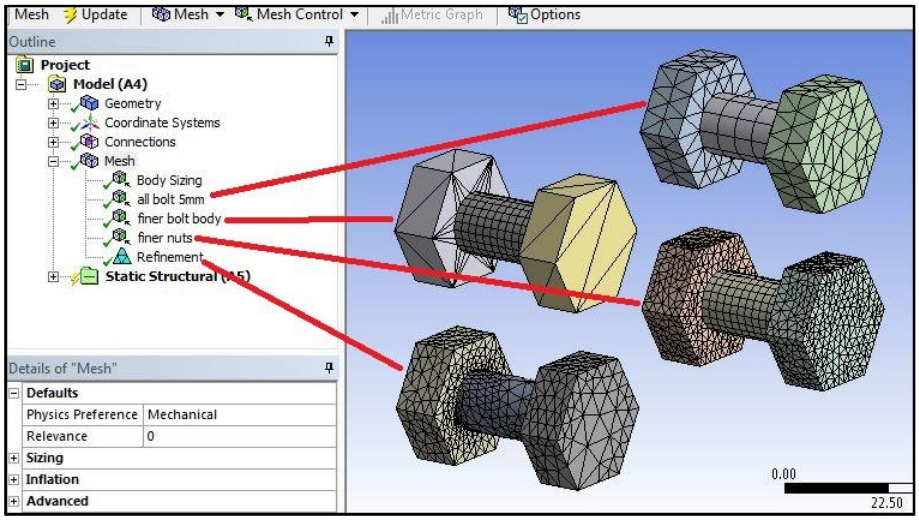

Figure 2.4 Different Meshing Options, ANSYS Workbench

In terms of meshing of bolts and the connecting parts, automatic meshing and independent body sizing options provided by ANSYS Workbench results in a coarse mesh as shown in Figure 2.5. With body sizing on the L-shaped angles, this region is meshed finer by using the refinement option, resulting in Figure 2.6. Similarly, the nuts could be independently meshed by body sizing and refinement options, and this effort results in the finer meshed angles and bolts as shown in Figure 2.7.

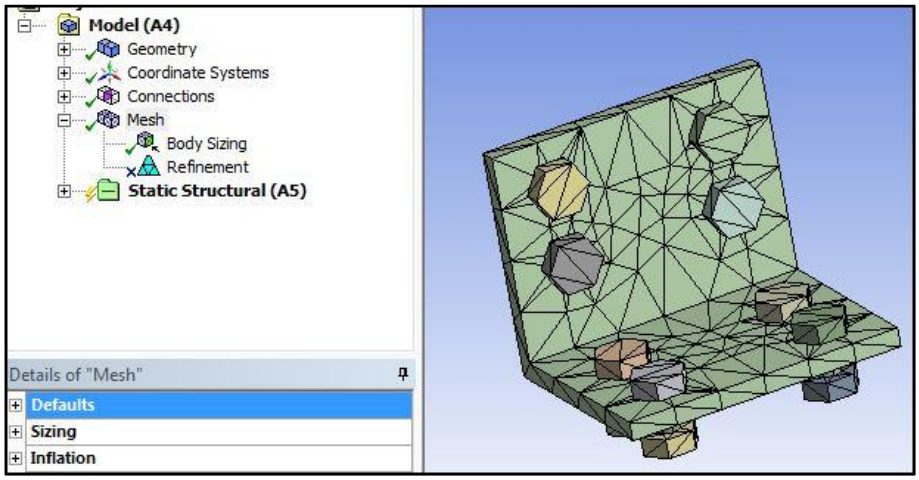

Figure 2.5 Profile – Bolt Connection (Default)

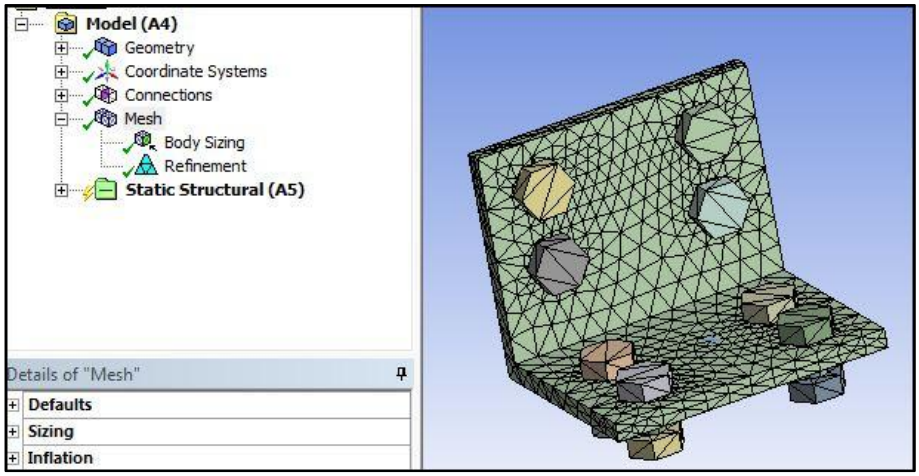

Figure 2.6 Profile – Bolt Connection (Refined L profile only)

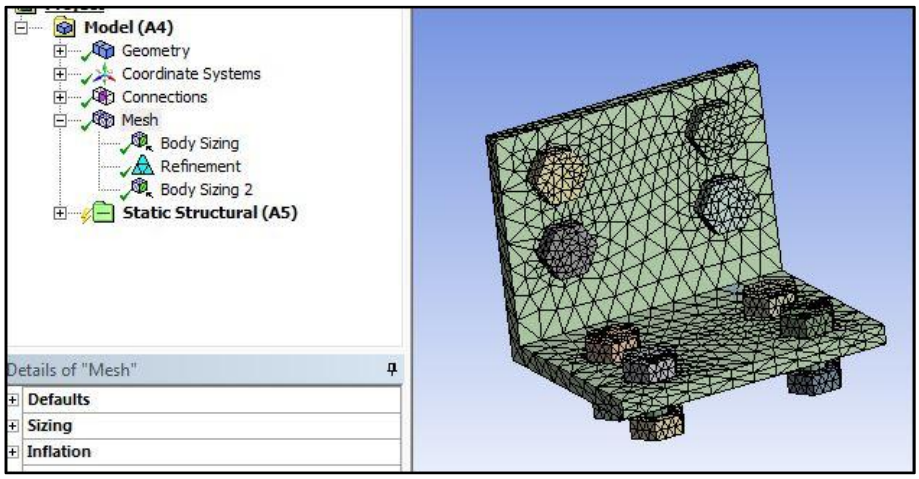

Figure 2.7 Profile – Bolt Connection (Refined L profile and bolts)

2.2.2 Meshing of L-Shaped Angles and I-Section Beam

In order to model the semi-rigid connection set up considered in this thesis, the connection region between the column face and beam end requires detailed meshing as explained in previous sections. Since the connection region also includes top and bottom angles and furthermore web angles connecting the beam to column face, these parts should also be meshed fine. On the other hand, the beam with I-section only transfers the forces acting at its end to the connection region, thus a coarser mesh can be chosen along the length of the beam after the connection region terminates. Additionally, the refinement property of the program is investigated on bolt sections in order to find out the accuracy of the results. The bolt's refinement meshing property have the positive effect on results but not effective enough. However, this little positive behavior of this meshing type is very effective on the computation time of overall.

In verification studies, it has been observed that refinement of the mesh along the remaining free part of the beam does not change the results but only increases the computation time. Three different beam body mesh options are considered on Azizinamini's 8S3 specimen (see Chapter 3 for details on this specimen), where fine meshed angles and coarse meshed I-section beam discretization option is shown in Figure 2.8. Moment-rotation curves for different meshed beam bodies are presented in Figure 2.9 and compared, and it is evident that further refinement on the beam body affects the results little with respect to the coarse mesh option on beam profile shown in Figure 2.8.

For bolts, L angles and back profile bodies, moment-rotation curves for three different meshing levels are presented in Figure 2.10 for Azizinamini's 8S3 specimen. The beam body mesh is kept constant and all remaining body meshing sizes are changed accordingly. It is evident that coarse meshing option results in large errors in the estimation of nonlinear response.

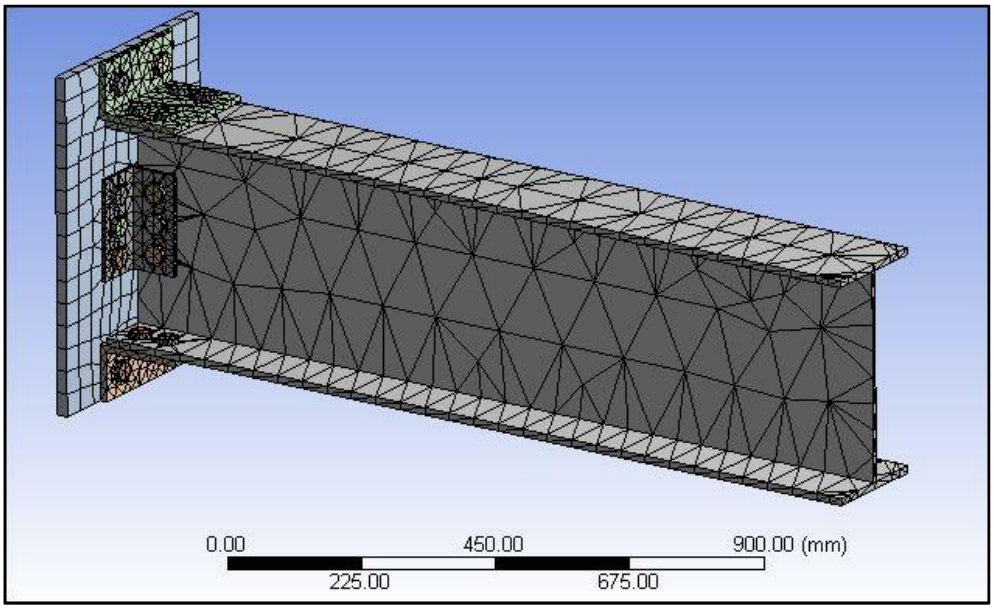

Figure 2.8 Coarse I-Section Beam – Fine Angles

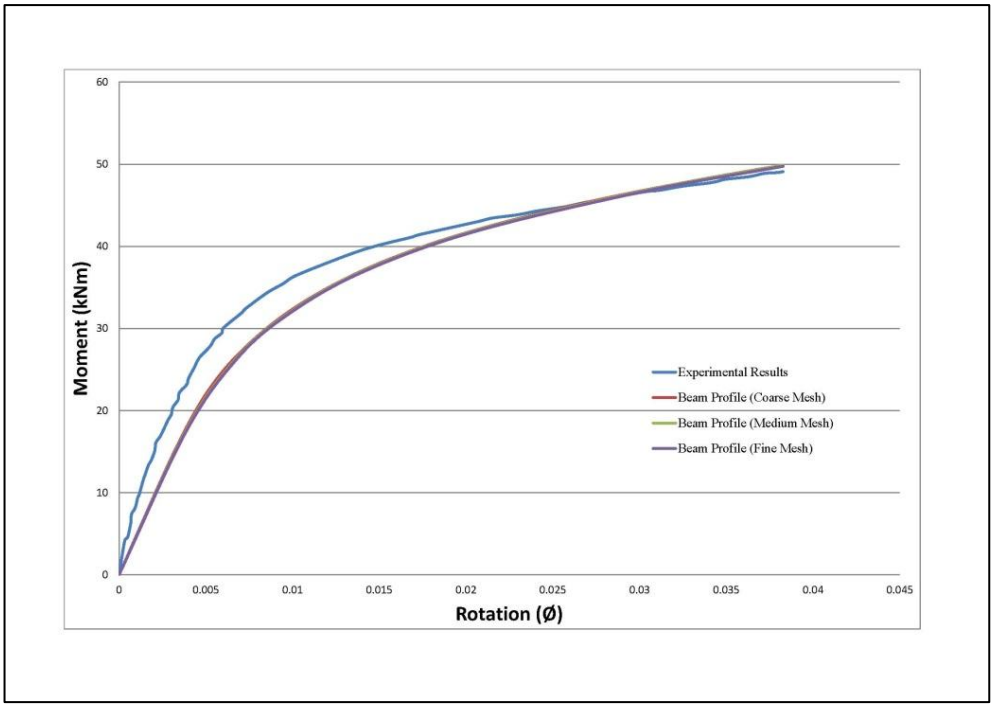

Figure 2.9 Beam Body Mesh Comparison Table

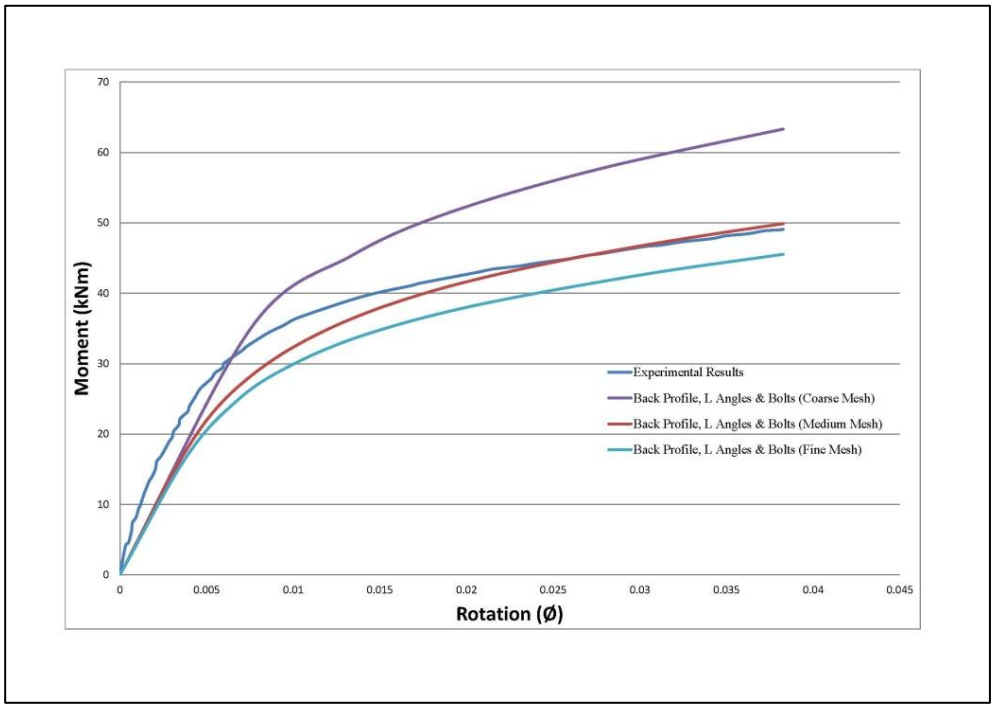

Figure 2.10 Back Profiles, L Angles & Bolts Meshing Comparison Table

2.3 Robustness of Simulations

Within the scope of this thesis, hundreds of trials have been conducted for the purpose of investigating the influence of meshing detail on the accuracy of results and furthermore on the computation times. In a finite element analysis, robustness is a crucial issue to take into account.

Computation times corresponding to various level of mesh refinement on different parts of the connection set up are given in Table 2.1. Meshing levels have been considered for following bodies: bolts, L-shaped angles, I-section beam, and column face. Analyses are conducted on an Intel Core i5 Processor with 2.50 GHz CPU and with 4 GB RAM regular notebook computer. During analysis trials, it has been observed that the optimum mesh selection is attained by considering coarse mesh on I-section beam and rest of the mesh medium refined.

Table 2.1 Approximate Time Consumption

Meshing Type	Bodies			Refinement at the Connection Parts	Analysis Type	Computation Time (Approximate)
	I Profile	L Angles	Bolts			
	Coarse	Coarse	Coarse	No	Monotonic	30 minutes - 1 hour
	Fine	Fine	Fine	No	Monotonic	6 hours – 12 hours
	Coarse	Fine	Fine	No	Monotonic	30 minutes – 3 hours
	Coarse	Fine	Fine	Yes	Monotonic	3 hours – 12 hours
	Coarse	Medium	Medium	Yes	Monotonic	30 minutes – 3 hours
	Coarse	Coarse	Coarse	No	Cyclic	24 hours – 72 hours
	Coarse	Fine	Fine	No	Cyclic	72 hours – 144 hours
	Fine	Fine	Fine	No	Cyclic	144 hours - … hours

During these trials, influence of cyclic loadings has been investigated, as well. It has been observed that cyclic analysis takes considerable amount of time even when the mesh level is coarse. In literature, to the knowledge of the author of this thesis, there is no research study published on the 3-D nonlinear cyclic analysis of even small structural systems that include material, geometric and contact nonlinearities. Evident from Table 2.1, such an analysis is computationally expensive first of all, then convergence issues cause further challenges when compared with monotonic analysis, and lastly accuracy attained from cyclic analysis cannot be easily verified due to lack of cyclic experimental data.

2.4 Nonlinear Contact Modeling Between Surfaces

Contact analysis is a naturally nonlinear phenomenon and description of contact between surfaces is therefore one of the most important parts of the modeling of semi-rigid connections through the use of advanced 3-D finite element programs. All contact bodies should be modeled independently and carefully so that the real physical behavior could be captured with sufficient accuracy in simulations.

In ANSYS, after the user finalizes drawing of the geometry of model, contact types should be defined. There are 5 different nonlinear types of contact options in ANSYS Workbench:

- **Bonded:** This is the default contact type in ANSYS Workbench. Gap opening/closing and furthermore sliding are not allowed in this contact type.
- **No Separation:** Gap opening/closing is not allowed as in bonded contact; however, sliding is allowed with friction coefficient equals to zero.
- **Frictionless:** Gap opening/closing is allowed and sliding is allowed with friction coefficient equals to zero.
- **Rough:** Gap opening/closing is allowed; sliding is not allowed and friction coefficient is set a large value by default through penalty formulation.
- **Frictional:** Gap opening/closing is allowed, and sliding is allowed if the sliding force is greater than the maximum static friction force that would develop between contact surfaces.

Frictional contact should be the type of contact to be used in steel semi-rigid connections and actually between all contact surfaces in other problems; since there is in reality always friction between all contact surfaces. It has been observed that frictionless and bonded solutions provide mostly much better convergences if the assumptions to use these contact types are valid under certain conditions. Due to the pretension present in the bolts, it has been observed that selection of frictional contact between all surfaces is not necessary and does not provide further accuracy in results.

In order to study the influence of friction coefficient on a simple structure, the following numerical setup shown in Figure 2.11 is prepared. The middle plate is pulled and the deformation value is measured from the bottom of middle plate. The numerical results obtained from varying the friction coefficient value between the plates are given in Figure 2.12. It is evident that the deformed shape of the setup matches with the expected physical shape. Furthermore, increases in the friction coefficient value result in successive increases in the nonlinear curves. It is suggested to conduct physical tests on steel surfaces with different smoothness properties and assess the accuracy of ANSYS in representing the frictional behavior of parts in the presence of material and geometric nonlinearities.

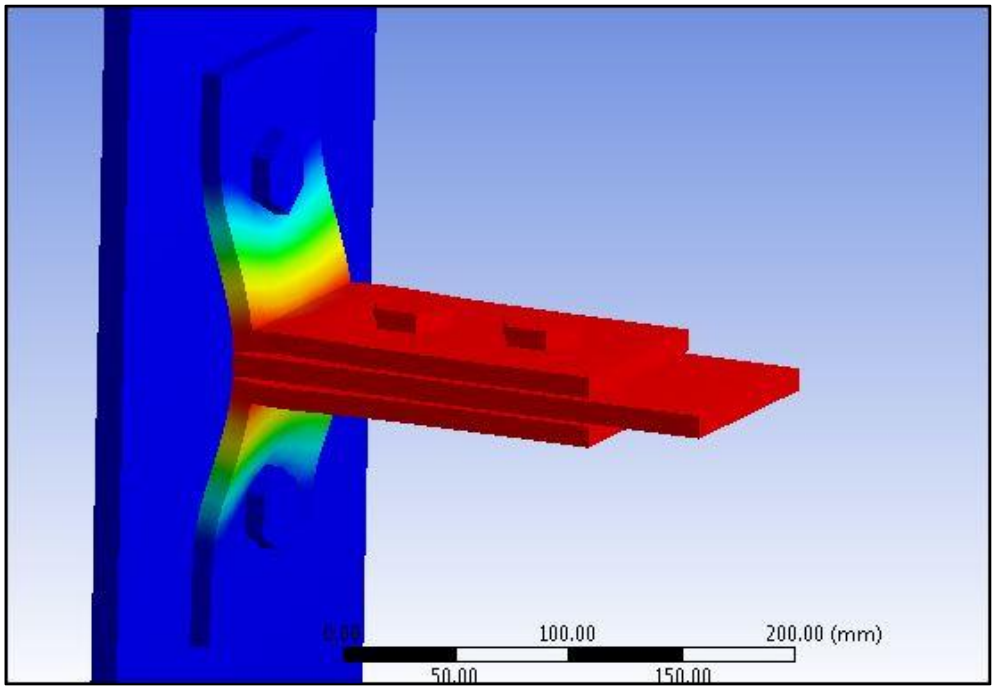

Figure 2.11 Numerical Test Setup for Friction Coefficient Comparison

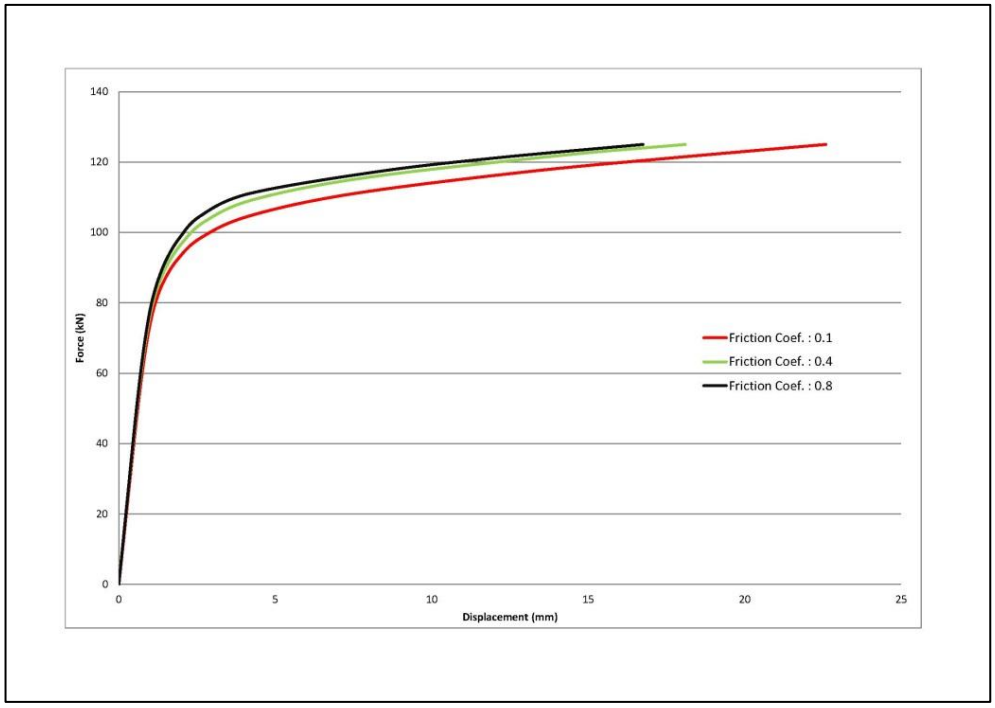

Figure 2.12 Influence of Friction Coefficient on Structure Response

2.4.1 Contact Simulation for Bolt Bearing

Most steel connections are manufactured with a hole that is greater than the bolt can fill in and the use of screws and opening screw threads in the plate are impractical especially if the plate gets thick. During loading of a plate to bolt connection, bearing stresses between the plate and bolt results in localized yielding in the plate's inner surface during contact, while the bolt remains elastic due to its high strength. Most manufactures try to avoid damage in the area of the hole and try to transform the shear forces between the bolt and plate through high friction forces caused due to bolt pretension. Obviously, it is also desired not to lose stiffness in the connection region due to the gap between the bolt and the plate, as well. In case that such a pretension is not provided, then simulation of this complex nonlinear phenomenon in ANSYS requires special definition of contact types between surfaces.

In this section, a demonstration example is considered in order to assess whether such localized bearing stresses are caused through proper definition of contact types. For this purpose, a plate with a hole is fixed at its side edges, and a bolt that passes through the hole is moved as it bears on the plate. Undeformed configuration of this example is shown in Figure 2.13.

Contact type between the surfaces is considered as frictional, and nodes on the bolt surface are considered as slave nodes in the contact definition of ANSYS and the nodes on plate's inner surface are considered as master nodes. As the two ends of the bolt presses on the plate in Figure 2.14, it has been observed that high bearing stresses are correctly localized at the contact point and stresses evolve through the contact region (Figure 2.15). It has been further observed that the initial diameter of the bolt hole increases due to the bearing action caused by bolt. Although not shown here, the bolt is also cyclically moved back and forth, and a proper description of the circular bolt region deforming on both directions has been captured.

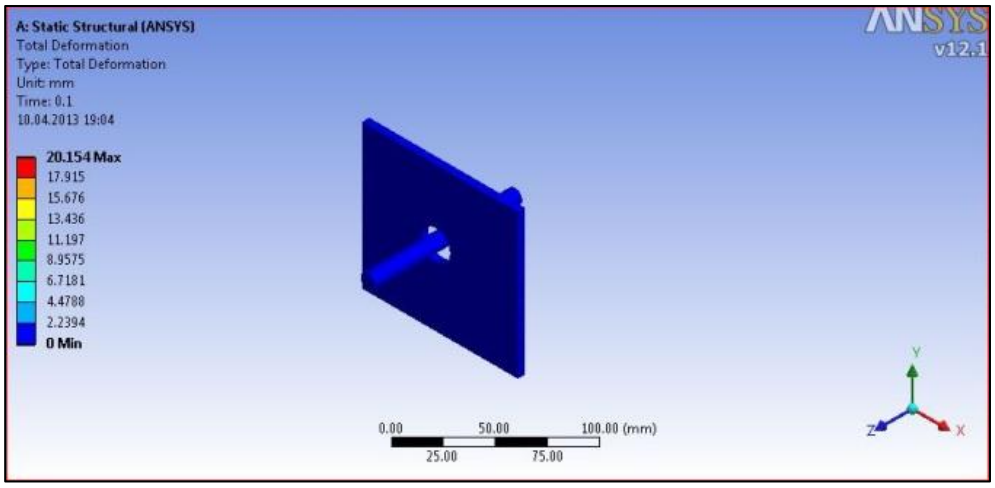

Figure 2.13 Undeformed shape of the profile for contact demonstration

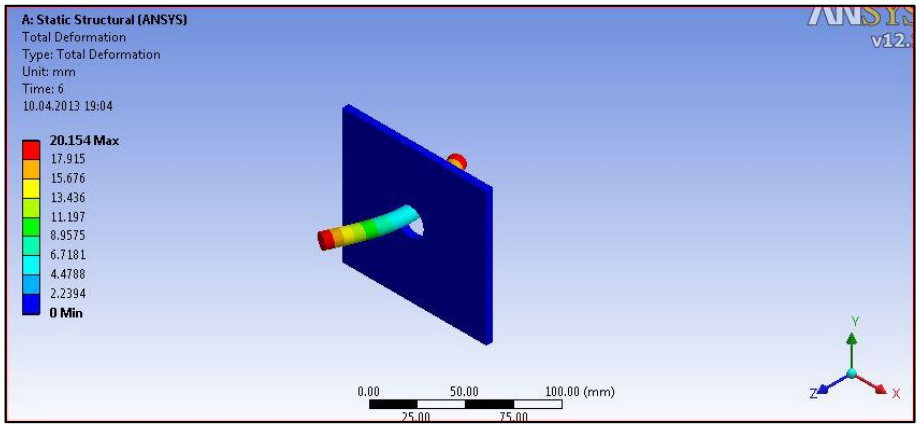

Figure 2.14 Deformed shape of the bolt for contact demonstration

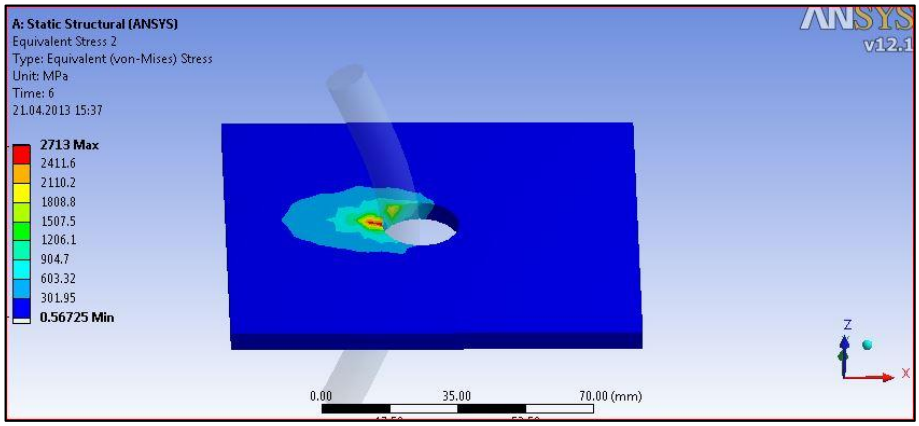

Figure 2.15 Stress Distribution of the profile for contact demonstration, ANSYS Workbench

2.5 Bolt Pretension

In order to define an accurate nonlinear behavior of semi-rigid connections, proper definition of bolt pretension is needed. As discussed above, bolt pretension provides transfer of shear forces acting on the bolt without damaging the area of the hole; thus, connection stiffness is increased from start of loading.

In ANSYS Workbench, pretension on a bolt can be provided in Static Structural module as shown in Figure 2.16.

As a demonstration of bolt pretension action, a U-shaped member made of steel is considered, where the side walls are connected through a bolt with nuts as shown in Figure 2.17. As pretension force initiates on the side walls, it is observed that the squeezing action is captured in the simulation in Figure 2.18.

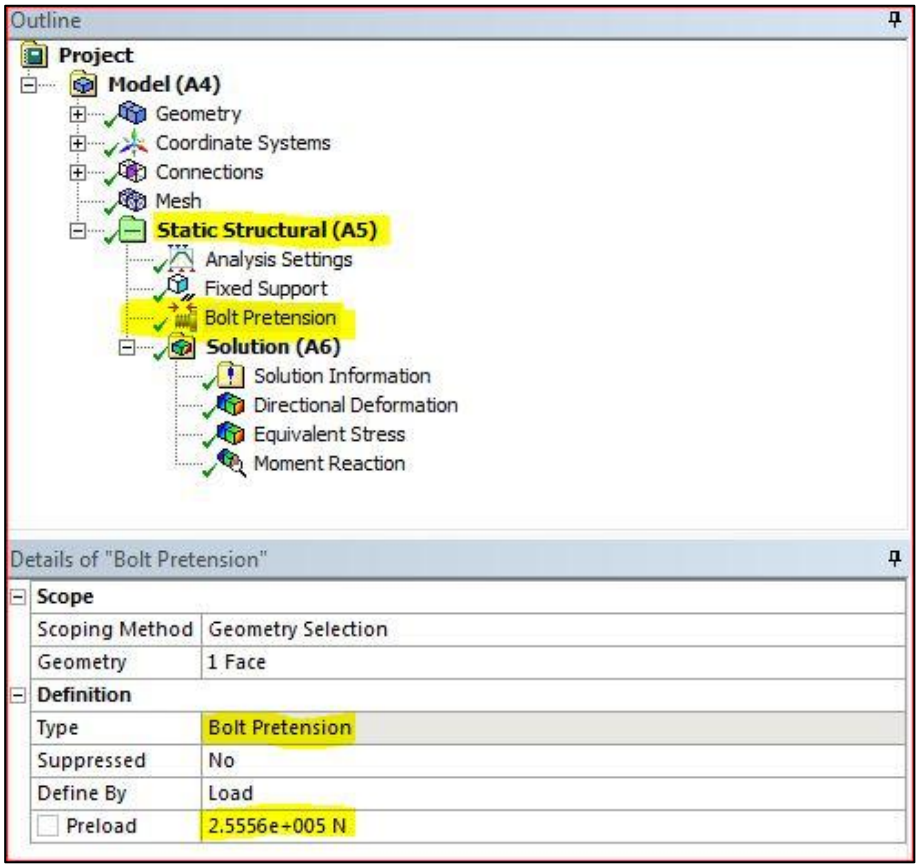

Figure 2.16 Static Structural Module of the ANSYS Workbench, ANSYS Workbench

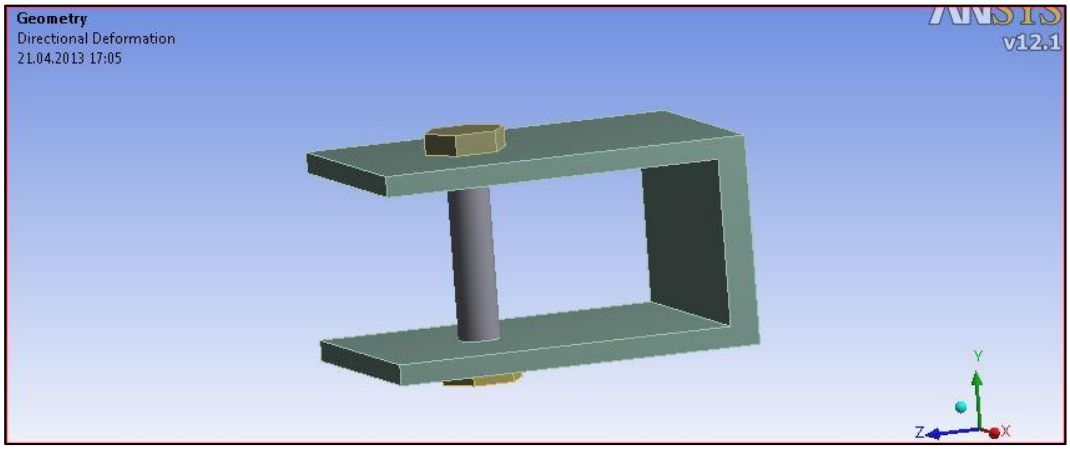

Figure 2.17 Undeformed Shape of U-Shaped Member for Bolt Pretension Demonstration

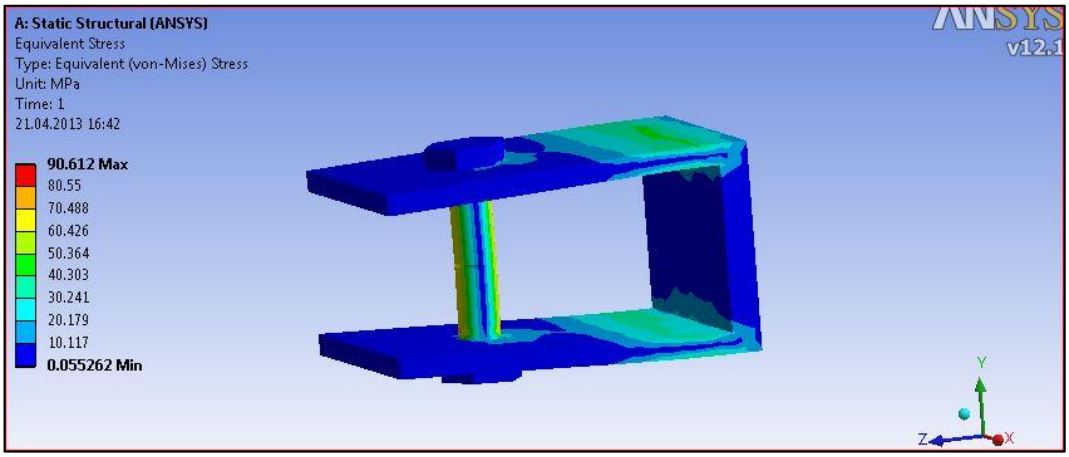

Figure 2.18 Deformed Shape of U-Shaped Member for Bolt Pretension Demonstration

CHAPTER 3

NONLINEAR FINITE ELEMENT MODELLING

In this chapter numerical simulations on top and seat angles with double web angles (TSADWA) connection by the use of ANSYS Workbench will be compared with experimental results of Azizinamini (1985), Calado et al. (2000) and Komuro et al. (2003). In this comparative study, all geometric and material properties used in ANSYS are taken from the experimental data provided in the tests. Utmost effort is given in terms of modeling all three different tests in a uniform manner by the use of ANSYS Workbench software.

3.1 Azizinamini's Experiments

Azizinamini (1985) in his Ph.D. study conducted experiments on TSADWA connection under mostly monotonic loading conditions, where some of the specimens were cyclically tested. This study was the first study carried out on TSADWA connection 50 years after the study by Rathbun (1936).

3.1.1 Material Properties

Grade of steel used in all connection parts, i.e. top, seat and web angles, and beam and column sections was ASTM A36 type. On these parts of the specimens, coupons were tested under uniaxial tensile loading and the material properties obtained from the tests were documented (Table 3.1). In the numerical study conducted in this thesis, average of the values in Table 3.1 are used for the calibration of steel material in the connecting angles and webs, as well as beam and column sections. In Azizinami's thesis, there was no information related to the material properties of the bolts, and for this reason the nominal properties reported for ASTM A325 heavy hex high strength type steel is considered.

Table 3.1 Azizinamini (1985) Coupon Test Results

Designation	Mechanical Properties		
	Yield Stress (ksi)	Ultimate Strength (ksi)	Elongation in 2-inch Gage Length (percent)
ASTM A36	42.8	69.9	23.8
	42.9	67.9	22.9
	39.3	68.0	32.5
	37.6	67.9	31.9
	36.5	71.9	31.3
	43.7	69.9	31.3
	40.0	64.0	34.4
	38.0	66.0	37.5

3.1.2 Test Specimens

Within the scope of this thesis, 5 different connection specimens from Azizinamini's tests were examined and compared with nonlinear finite element simulation results. Tag number and geometric properties of these specimens are listed in Table 3.2. 8Sx type specimens had smaller beam cross sections compared to 14Sx specimens, and consequently less stiffness and moment carrying capacities, as well. In all specimens shown in Table 3.2, 7/8 and 3/4 inches diameter bolts were used.

Table 3.2 Specimens of Azizinamini (1985) used in FE Simulations

Specimen Number	Type of Test	Beam Section	Top & Bottom Flange Angles			Web Angles	
			Angle	Length (inches)	Bolt Spacing (inches)	Angle	Length (inches)
8S1	Static	W8x21	L 6x3.5x0.3125	6	3.5	2 x L4x3.5x0.25	5.5
8S2	Static	W8x21	L 6x3.5x0.375	6	3.5	2 x L4x3.5x0.25	5.5
8S3	Static	W8x21	L 6x3.5x0.3125	8	3.5	2 x L4x3.5x0.25	5.5
14S1	Static	W14x38	L 6x4x0.375	8	5.5	2 x L4x3.5x0.25	8.5
14S5	Static	W14x38	L 6x4x0.375	8	5.5	2 x L4x3.5x0.25	8.5

Experimental set up of the tests is shown in Figure 3.1 and Figure 3.2 for 8Sx and 14Sx specimens, respectively. In order to save time, the symmetry about the centroid of the

test set up is taken into account. In the finite element model, the back face of the column flange is assumed to be fixed supported and the end of the beam profile is displaced in the transverse direction (Figure 3.3).

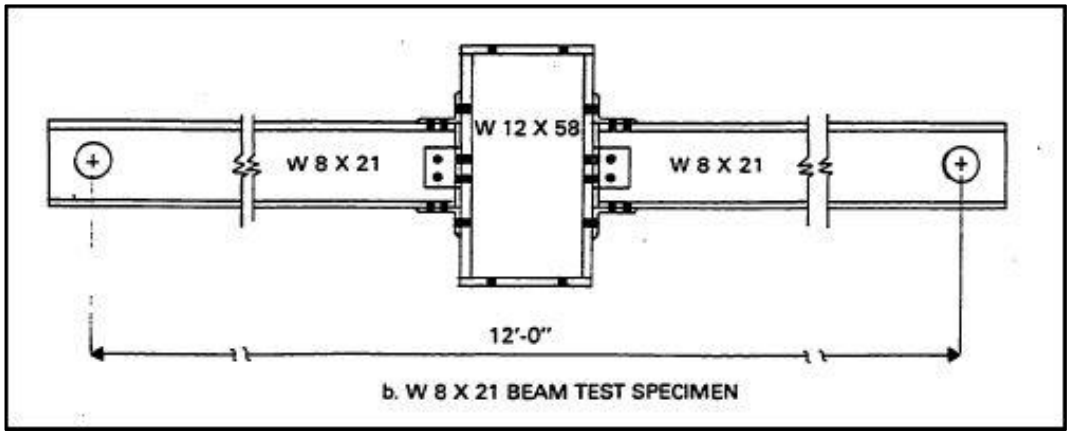

Figure 3.1 8sx Test Specimen Setup, Azizinamini (1985)

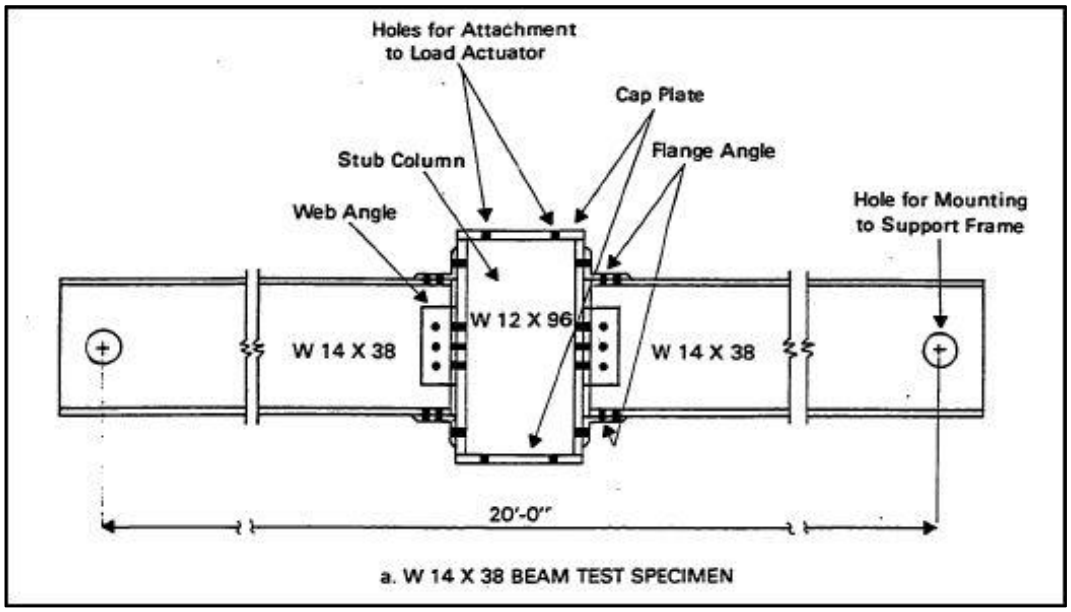

Figure 3.2 14sxTest Specimen Setup, Azizinamini (1985)

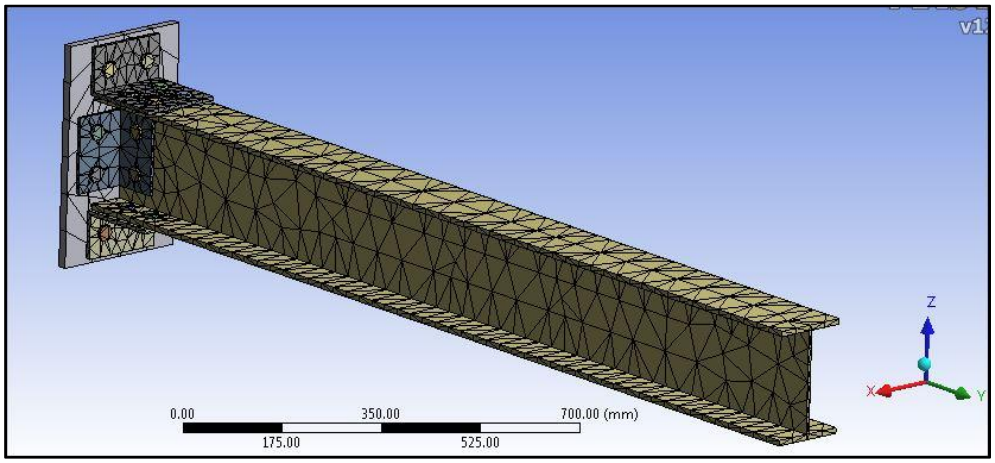

Figure 3.3 Nonlinear Undeformed Finite Element Model for 8S1

With regards to the modeling and meshing strategy employed for the test specimens in numerical environment, detailed information is available in Chapter 2. As a summary, all contact surfaces between the connecting parts, bolt pretension, friction values, and nonlinear material definitions for steel are provided in ANSYS Workbench. The expected deformed shape of the connection region, i.e. the column face connecting to the beam through angles and bolts, is demonstrated pictorially in Azizinamini's study (Figure 3.4). Due to downward movement of the beam, the top angle is expected to deform significantly and a gap would open up there, and the bottom angle profile is expected to be compressed. The finite element model set up in this thesis has successfully captured this physical action, as shown for specimen 14S5 in Figure 3.5.

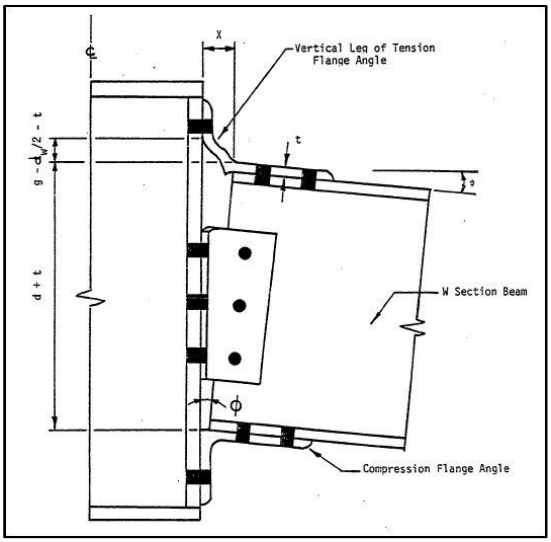

Figure 3.4 Expected Deformed Shape, Azizinamini (1985)

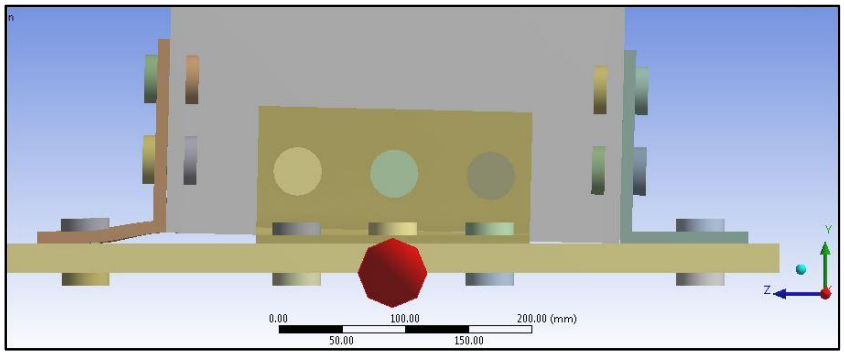

Figure 3.5 Nonlinear Deformed Finite Element Model for 14S5

The moment-rotation curves obtained from the numerical simulations is compared next with the experimental moment-rotation curves for the specimens listed in Table 3.2.

The first comparison regarding to Azizinamini's tests is for 14S1 specimen. The bolts connecting this specimen is loaded first with a 250 kN pretension force, and 0.1 friction coefficient is used on all steel surfaces. The numbers of nodes and elements used for the simulation of 14S1 specimen were 55,287 and 20,305, respectively. All modeling and meshing details could be found in Chapter 2.

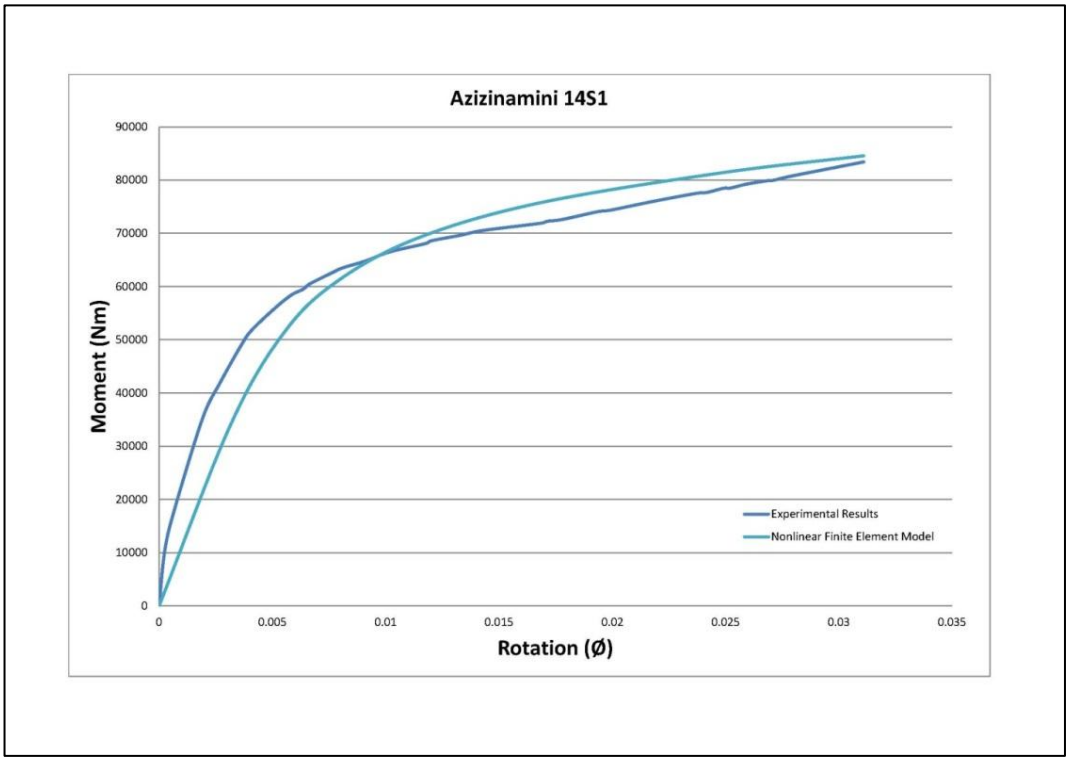

Figure 3.6 Comparison of Moment-Rotation Responses for 14S1 Specimen of Azizinamini

As can be easily seen in Figure 3.6, moment-rotation curve obtained from numerical simulation provides a good overall match with experimental data; however there is a

discrepancy observed in the initial stiffness of the connection. Furthermore, slight overestimation of plastic moment capacity of connection is also evident in the plot. Undeformed and deformed shapes of the finite element model could be found in Appendix A. Evident from these results, the physical actions that occurred in this specimen was satisfactorily simulated through the detailed modeling of the connection region in ANSYS Workbench.

Second comparison from Azizinamini tests is for 14S5 specimen. As presented in Table 3.2, W14x38 type of beam (I profile) is used with 6 × 4 × 0.375 inches top and bottom angles (L profiles) and 4 × 3.5 × 0.25 inches web angles. 250 kN pretension value is given on the bolts and 0.1 value of friction is applied between surfaces. 81,560 nodes and 27,649 elements were used in order to model 14S5 specimen. 14S1 and 14S5 specimens are exactly the same except than the difference in bolt diameters. 0.75 inch diameter bolts were used in 14S1 and 0.875 inch diameter bolts were used in 14S5.

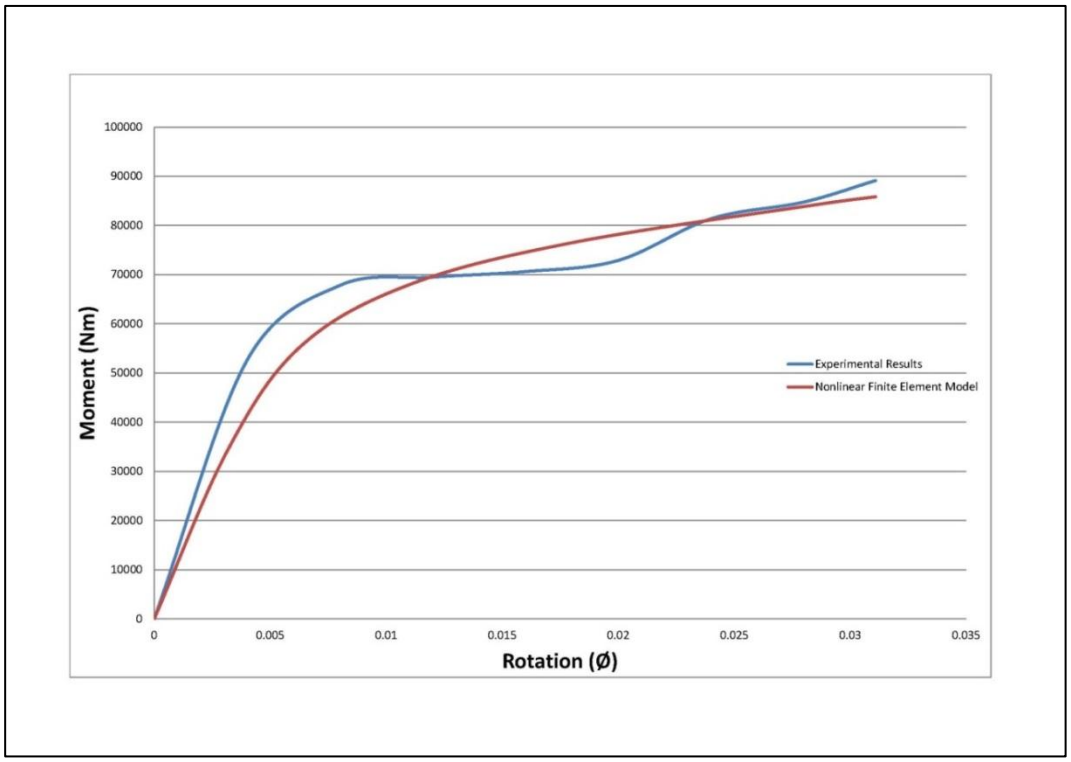

Figure 3.7 Comparison of Moment-Rotation Responses for 14S5 Specimen of Azizinamini

With larger diameter bolts, 14S5 specimen is expected to have a larger moment capacity compared to 14S1 specimen. Both the experimental and the numerical results clearly indicate this expected strength increase in the connection region as seen in Figure 3.7. Similar to 14S1 specimen results, the numerical simulation underestimated the initial stiffness of the connection response, but very close overall match is observed with the experimental data when the whole moment-rotation curves are compared. Undeformed and deformed finite element models of this specimen are presented in Appendix A.

Concluding on the numerical results with that of experimental results of 14Sx specimens, it is observed that good match is obtained in overall responses and the use of ANSYS Workbench finite element program in this regards was satisfactory and the capabilities of this software package to simulate complex nonlinearities in the connection region is sufficient.

In the second group of Azizinamini's tests, i.e. 8Sx type specimens, W8x21 type of beams (I profiles) were used in the experimental set up (Table 3.2). In this thesis, three of the 8Sx specimens are considered for modeling in ANSYS; where the web angles of these specimens had the same dimensions, i.e. 2×L4 × 3.5 × 0.25 inches L profiles with 5.5 inches length, and L 6 x 3.5 x 0.3125 inches top and bottom angles with 6 inches length. Azizinamini's test setup was presented in Figure 3.2 and the finite element model for undeformed shape could be found in Appendix A. In ANSYS model, 175 kN pretension force was applied on the bolts for 8S1 specimen. 18,799 nodes and 7,994 elements were used in order to model this specimen in ANSYS.

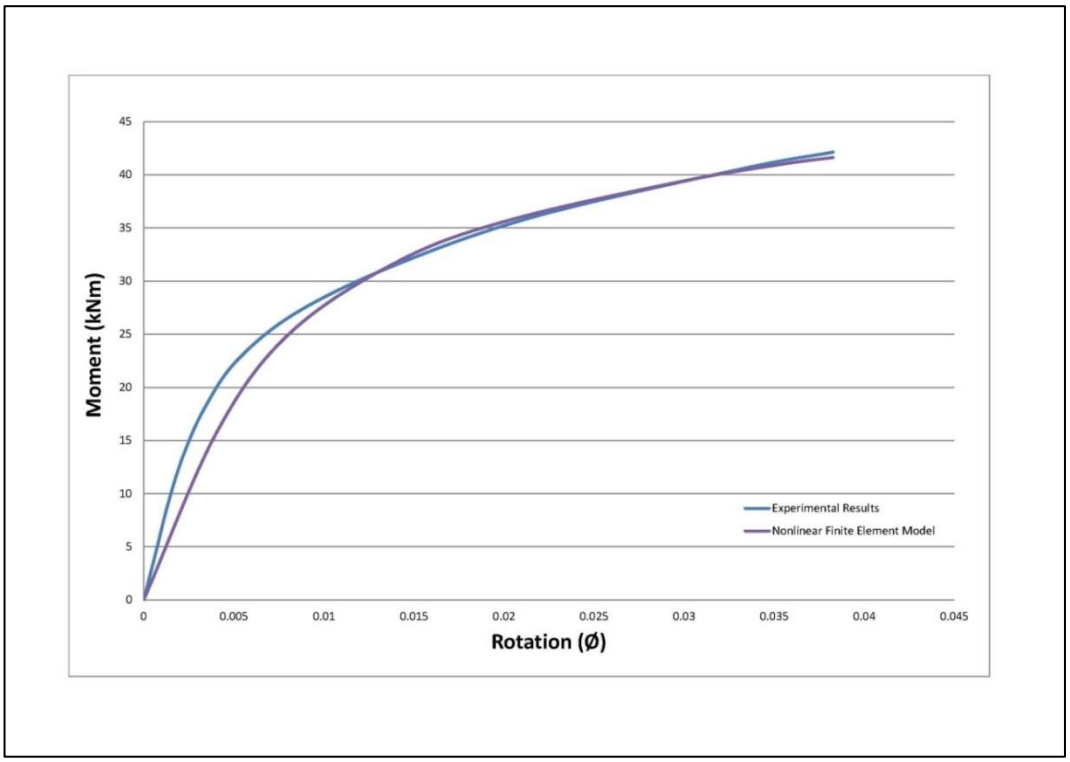

Figure 3.8 Comparison of Moment-Rotation Responses for 8S1 Specimen of Azizinamini

Comparison of the numerical and experimental moment-rotation curves reveal similar patterns as observed in 14Sx specimens. The initial stiffness of the connection is underestimated, but this time the plastic moment capacity is perfectly captured, and the

overall comparison of both moment-rotation curves indicate good match. The deformed shape of the nonlinear finite element model could be found in Appendix A.

Second comparison from Azizinamini 8Sx tests is for 8S2 specimen, where the web angles had the same dimensions with 8S1 that is 2 × L 4 × 3.5 × 0.25 inches with 5.5 inches length. The top and bottom angles (L profiles) have 2 x L 6 x 3.5 x 0.375 inches with 6 inches length. For 8S2 specimen, 175 kN pretension force is applied on the bolts as done for 8S1 specimen. 24,930 nodes and 9,947 elements were used in order to model the nonlinear behavior of 8S2 specimen in ANSYS.

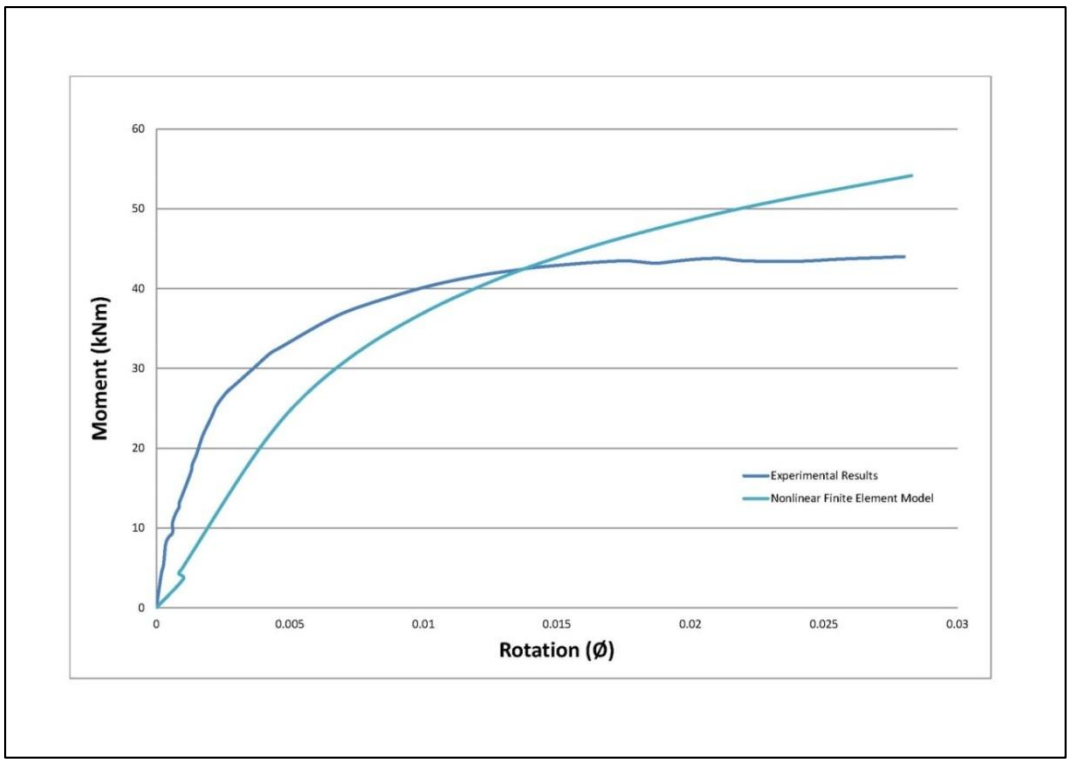

Figure 3.9 Comparison of Moment-Rotation Responses for 8S2 Specimen of Azizinamini

Moment-rotation response obtained from numerical simulation for 8S2 specimen is compared with the experimental data in Figure 3.9. Among all specimens analyzed and modeled from Azizinamini's tests, the largest deviation between the experimental and numerical results occurred in this specimen. Similar to other specimen results, the initial stiffness is underestimated, but this time the plastic moment capacity is overestimated with much larger error compared to other specimen results. The deformed shape of the nonlinear finite element model could be found in Appendix A.

The last specimen considered among 8Sx group of specimens is 8S3. As mentioned before, the web angles had the same dimensions with 8S1 & 8S2 specimens, i.e. 2 × L 4 ×

3.5 × 0.25 inches with 5.5 inches length. The top and bottom angles (L profiles) have dimensions 2 × L 6 × 3.5 × 0.3125 inches with 8 inches length. For 8S3 specimen, 175 kN pretension force is applied on the bolts as done similarly for 8S1 and 8S2 specimens. 24,947 nodes and 10,204 elements were used in order to model 8S3 in ANSYS.

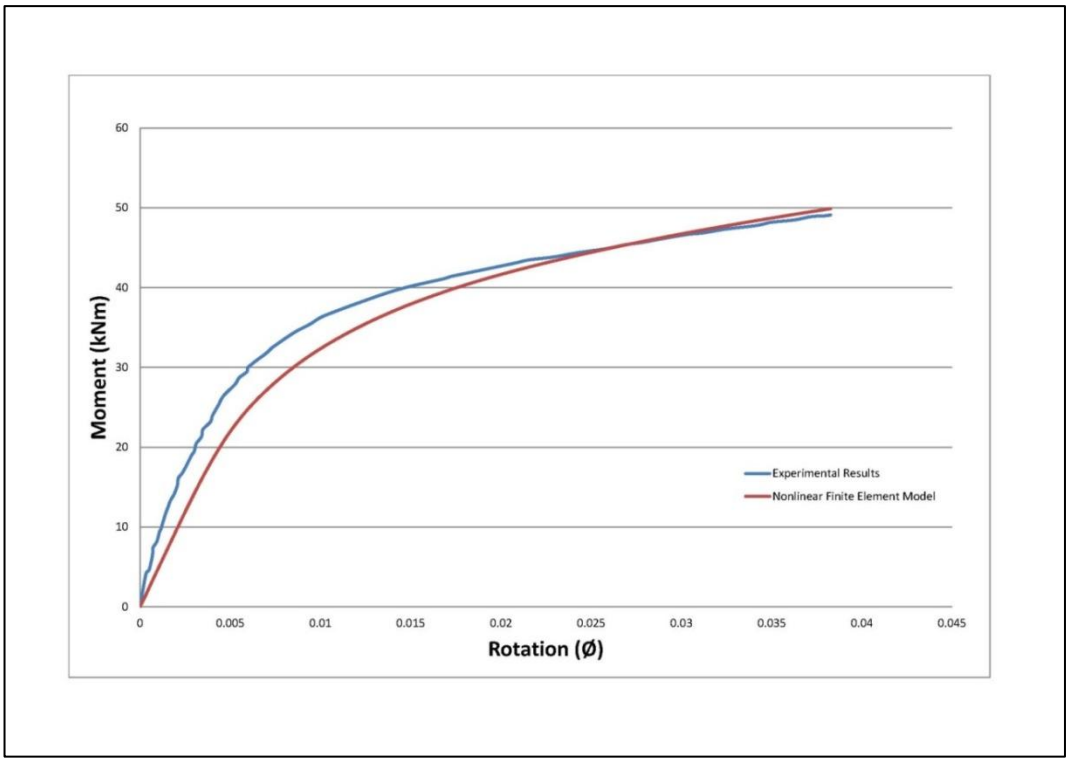

Figure 3.10 Moment-Rotation Responses for 8S3 Specimen of Azizinamini

Moment-rotation response obtained from numerical simulation for 8S3 specimen is compared with the experimental data in Figure 3.10. The numerical simulation of 8S3 specimen provides good match compared with the experimental data, where only the initial stiffness is underestimated but the plastic moment capacity is perfectly captured as in the case of 8S1 specimen. The deformed shape of the nonlinear finite element model could be found in Appendix A.

As a summary of the numerical simulations on Azizinamini's 14Sx and 8Sx specimens, good match is obtained in terms of tracing the nonlinear moment-rotation curves. Discrepancies in numerical and experimental results exist especially in the initial stiffness, and overall plastic moment capacities are mostly captured with great accuracy. Close match attained from numerical models indicate sufficient capture of the physical actions present in the connection region, where this is also verified with the simulated deformed shapes of the connection region of the specimens.

3.2 Calado's Experiments

15 years after Azizinamini's tests, Calado et al. (2000) published their experimental study on semi rigid connections. In their tests, they used three different specimen sizes and in total conducted 15 tests on top and seat angles with double web angles (TSADWA) connection. Among each specimen group, one monotonic loading test and four cyclic loading tests were conducted. The main purpose of their study was to increase the experimental database on TSADWA connection and furthermore carry out both monotonic and cyclic load tests in order to assess the influence of cyclic loading on connection response.

3.2.1 Material Properties

Calado et al. (2000) conducted their tests in Material and Structures Test Laboratory of the Instituto Superior Technico of Lisbon, Portugal. In their tests, S 235 JR grade of steel was used for solid bodies like L angles, I profiles and columns. In order to document the mechanical properties of the steel, two coupon tests were performed on each body part. The results of the coupon tests are provided in Table 3.3 and Figure 3.11. Similar to Azizinamini's test data documentation, Calado et.al. did not provide material properties on bolts, where the only information on them was the fact that they were 8.8-M bolts.

Table 3.3 Material Properties of the Specimens, Calado et al. (2000)

Member Section	Section Element	f_y (Mpa)	ε_y (%)	f_u (Mpa)	ε_t (%)
HEB 160	web	348.63	0.53	490.31	31.5
	flange	303.41	0.84	453.12	44.5
HEB 200	web	302.31	0.55	434.39	38.2
	flange	282.29	0.75	433.27	43.3
HEB 240	web	290.28	0.52	447.91	39.6
	flange	304.74	0.81	454.4	39.1
IPE 300	web	215.67	0.66	451.26	41.1
	flange	304.71	0.68	452.63	42.7
L 120 x 10	-	252.23	0.52	420.14	44.5

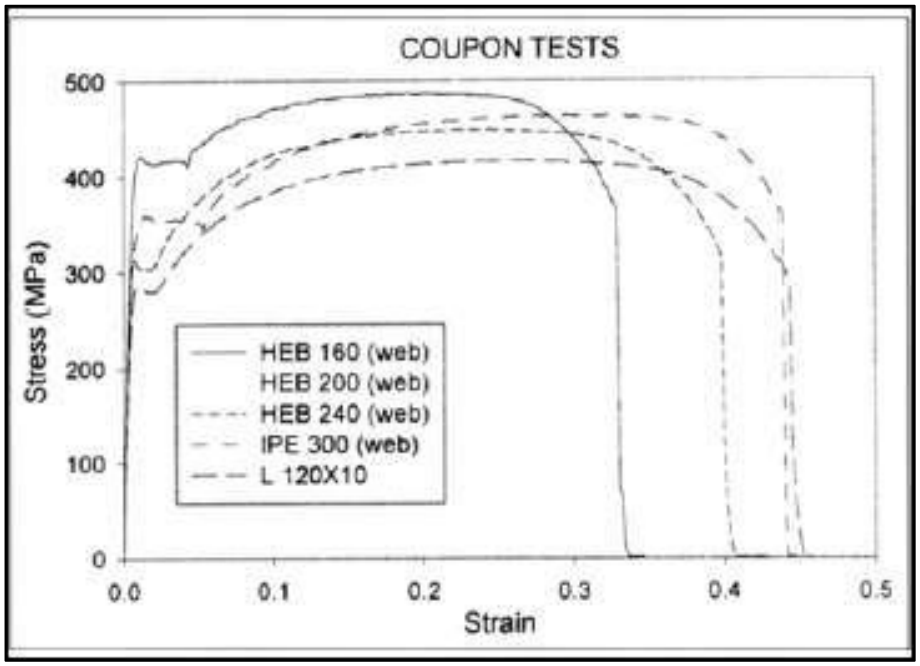

Figure 3.11 Coupon Test Results of the Specimens, Calado et al. (2000)

3.2.2 Test Specimens

Within the scope of this thesis, all specimens tested monotonically by Calado et al. (2000) are considered for numerical modeling and simulation in ANSYS. The specimens are listed below in Table 3.4 and also presented in Figure 3.12.

IPE 300 type of beams (I profiles) were used in the tests with two top and bottom L angles with 120×120×10mm dimension and two web angles with L 120×80×10mm dimension. The column profile dimensions are variable as expressed in Table 3.4. The test setup and dimensions are presented in Figure 3.13, where IPE 300 type beam member is connected to the column profiles with the help of the two identical top and bottom angles and two identical web angles. The system is designed symmetrically. While connecting the top and bottom angles to the column and I profile, the 8.8 quality M16 bolts were used and for the web angles, 3 bolts with 8.8 quality were used.

Despite the lack of material data on the bolts, the value of pretension force applied on the bolts was provided by Calado et al. (2000), and it was 88 kN. It has to be reminded that in Azizinamini's tests, no data on bolts was available, both for material properties and pretension force. Since the pretension force on the bolts was available for Calado specimens, that value is first applied on the bolts in the numerical model in ANSYS. The value of friction coefficient was not available in the paper by Calado, therefore it was taken as the same used in Azizinamini's tests.

Table 3.4 Specimen Table for Calado et al. (2000)

Specimen Number	Type of Test	Beam Section	Top & Bottom Flange Angles (mm)	Web Angles (mm)	Column Section
BCC7	Static	IPE300	L 120x120x10	L 120x80x10	HEB 200
BCC9	Static	IPE300	L 120x120x10	L 120x80x10	HEB 160
BCC10	Static	IPE300	L 120x120x10	L 120x80x10	HEB 240

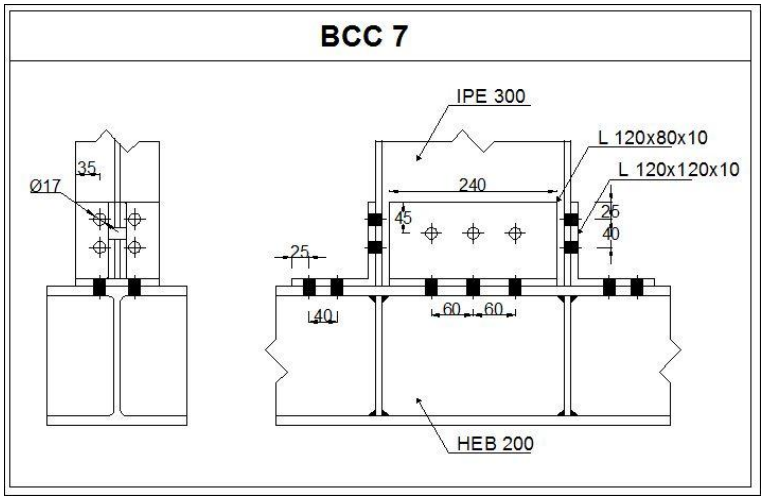

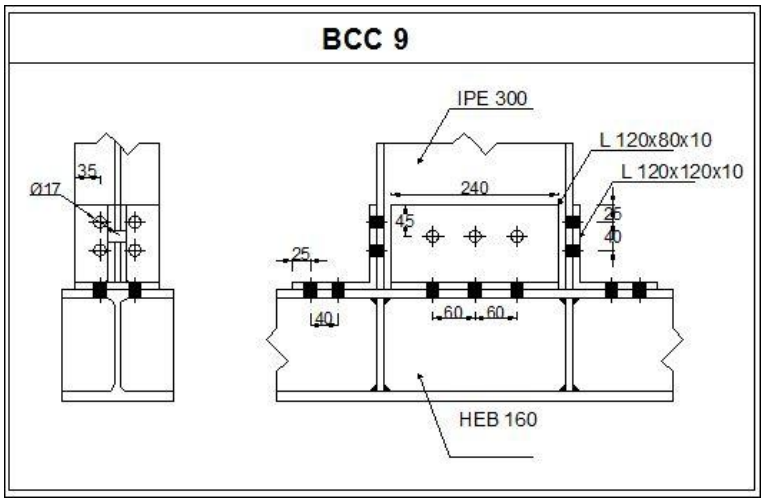

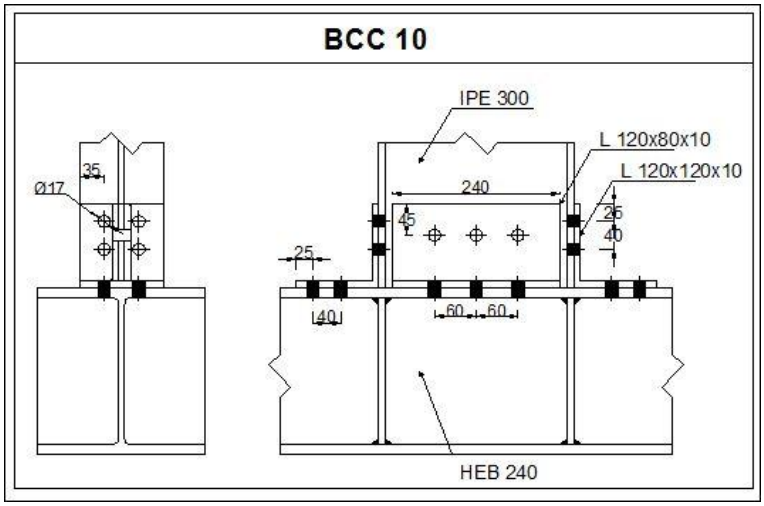

Figure 3.12 Experimental Test Setups for the Specimens, Calado et al. (2000)

Calado et al. (2000) applied a displacement from the end of the beam section as seen in Figure 3.13 and plotted the moment-rotation results in terms of moment calculated from the measured force at load application multiplied by the distance between the load application point and the centroid of the column section that is connected to the beam element. In their paper, it was argued that such a plot is a common way of representing the moment-rotation behavior of connections. This calculation procedure is also followed in plotting the moment-rotation results of the numerical simulations.

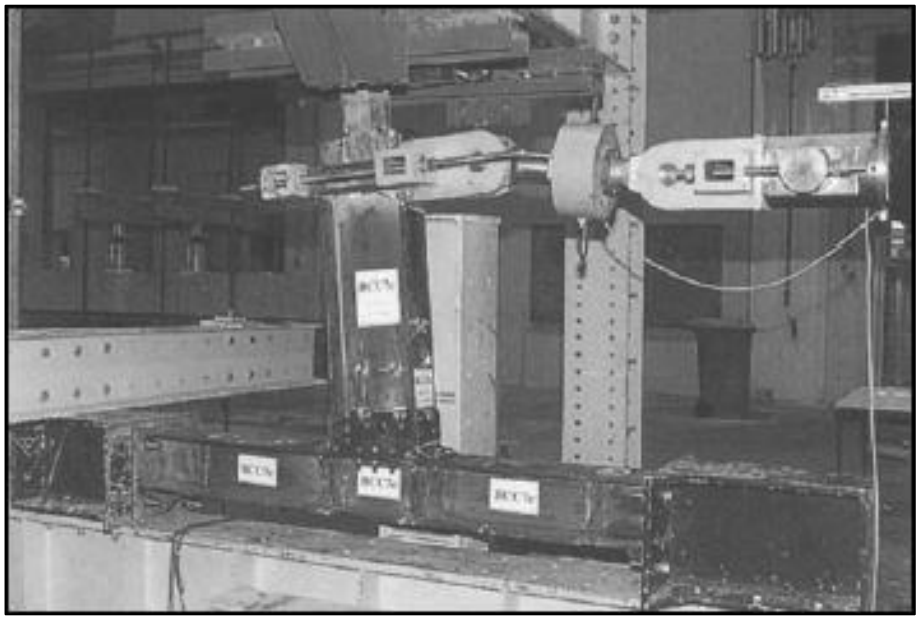

Figure 3.13 Testing Lay-out, Calado et al. (2000)

The whole beam profile (IPE 300) is modeled in ANSYS and only the upper flange of the column profile is modeled as a thick plate providing restraint at the end as seen in Figure 3.14, where the back faces of the column top flanges were fixed.

The first verification of the numerically simulated specimens is the presentation of the deformed shapes. Comparison of the deformed shape obtained from finite element model in Figure 3.15 presents good match with the experimental ones shown in

Figure 3.16, proving the sufficiency of the numerical model in capturing the physical deformations present in the connection region. At the end of loading, significant opening is created in top angle profile and the bottom angle profile presses on the column flange.

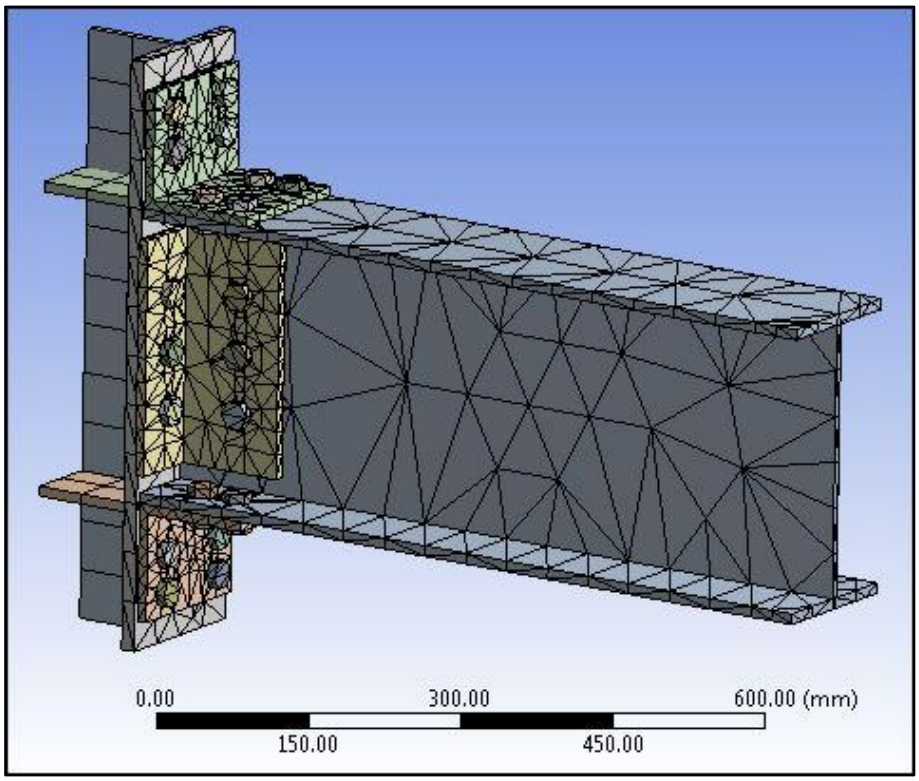

Figure 3.14 Undeformed Shape of model for BCC7

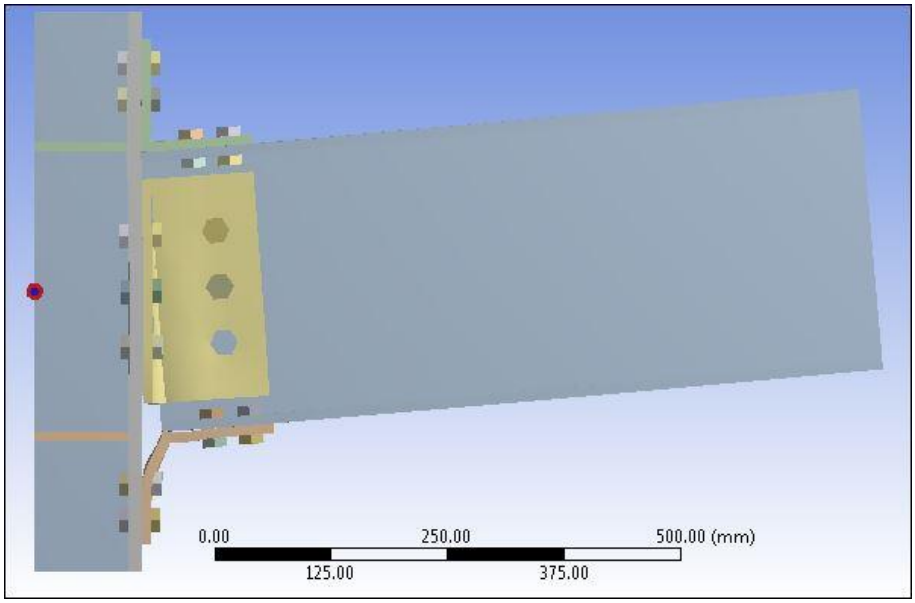

Figure 3.15 Deformed Shape of model for BCC7

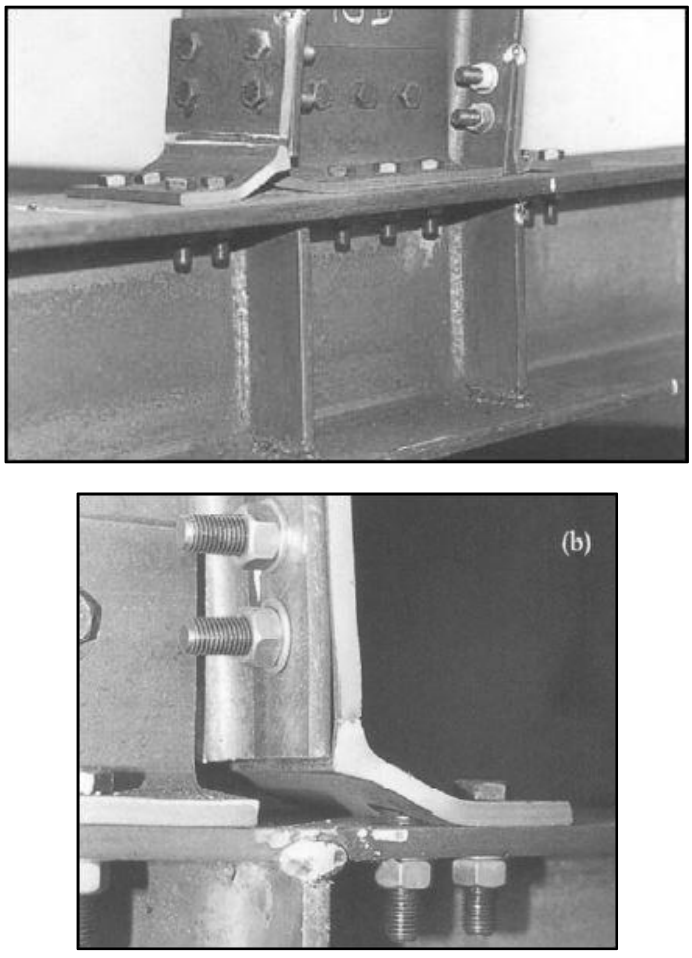

Figure 3.16 Deformed Shape of Experimental Test Setup

The first specimen compared among Calado et al. (2000)'s monotonic tests is specimen BCC7. As presented in Table 3.4, IPE 300 type of beam is used for this specimen with HEB 200 column section, 2 × L120×120×10mm top and bottom angles and 2 × L120×80×10mm web angles. In terms of bolts, 8.8 quality M16 bolts were used in the experiments as mentioned before and the bolts were loaded with 88 kN pretension force first before loading laterally. 24,094 nodes and 10,108 elements were used in order to model the nonlinear behavior of BCC7 specimen in ANSYS.

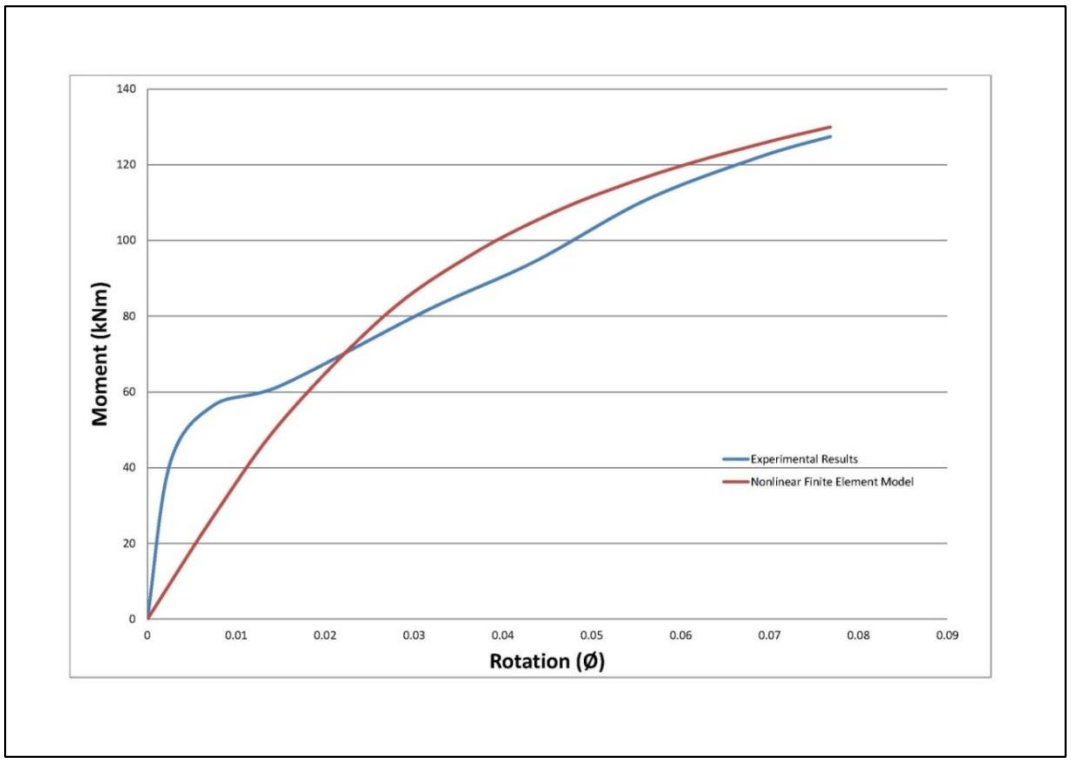

Figure 3.17 Comparison of Moment-Rotation Responses for BCC7 Specimen of Calado et al. (2000)

When experimental results are compared with the finite element results as presented in Figure 3.17, significant underestimation of the initial elastic stiffness is evident in the plot of numerical results. This discrepancy can be closed with increased pretension force applied on the bolts, but such an approach was not followed in this thesis, since the pretension force was documented in Calado et al. (2000)'s tests and that value was used the same in order to be consistent. It is also worth to mention that increasing pretension force excessively also causes premature yielding of the connecting parts, and this leads to an undesired failure of the connection region. Despite the discrepancy in the initial stiffness, the final plastic moment capacity of the connection is accurately capture with the finite element model analysis. Furthermore, the deformed shape of the specimen clearly shows correct physical action in the connection region as shown in Appendix A.

The second comparison is conducted on BCC9 specimen of Calado et al. (2000). As presented in Table 3.4, IPE 300 type of beam was used with HEB 160 column section, 2 × L120×120×10mm top and bottom angles and 2 × L120×80×10mm web angles. 8.8 quality

bolts with M16 dimension were used and 88 kN pretension force is applied in the numerical model as done in the experiment. 21,884 nodes and 7,984 elements were used in order to model BCC9 specimen in ANSYS.

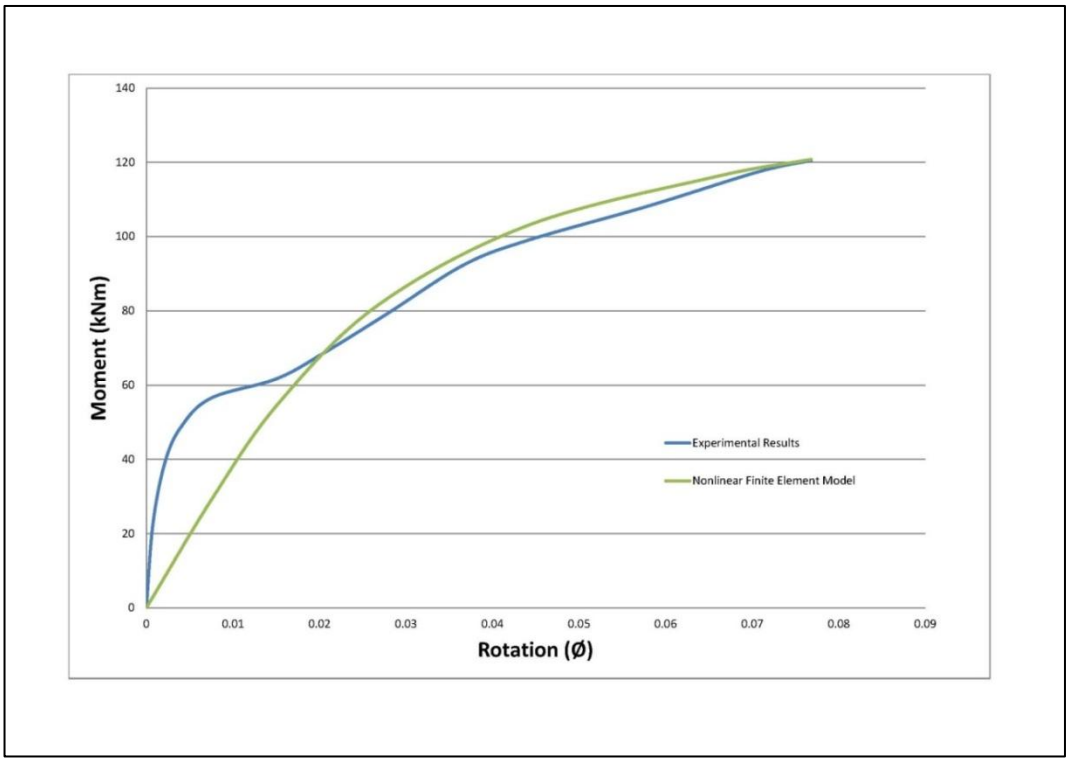

Figure 3.18 Comparison of Moment-Rotation Responses for BCC9 Specimen of Calado et al. (2000)

Moment-rotation response obtained from finite element simulation of BCC9 specimen is compared with the experimental data in Figure 3.18. It is evident that similar to BCC7 specimen, initial stiffness is overly underestimated, yet the final plastic moment capacity is still close to the experimental data. Undeformed and deformed shapes of the finite element models for BCC9 specimen could be found in Appendix A.

The final specimen used for comparison is BCC10 from Calado et al. (2000)'s tests. In this specimen, HEB 240 type of column profile was used, resulting in increased moment-rotation behavior. 8.8 quality M16 bolts were used on 2 × L120×120×10mm top and bottom angles and 2 × L120×80×10mm web angles. 88 kN pretension force was applied on the bolts before lateral loading. 22,555 nodes and 7,946 elements were used in order to model BCC10 specimen in ANSYS, i.e. same discretization is employed between all simulated specimens of Calado et al. (2000).

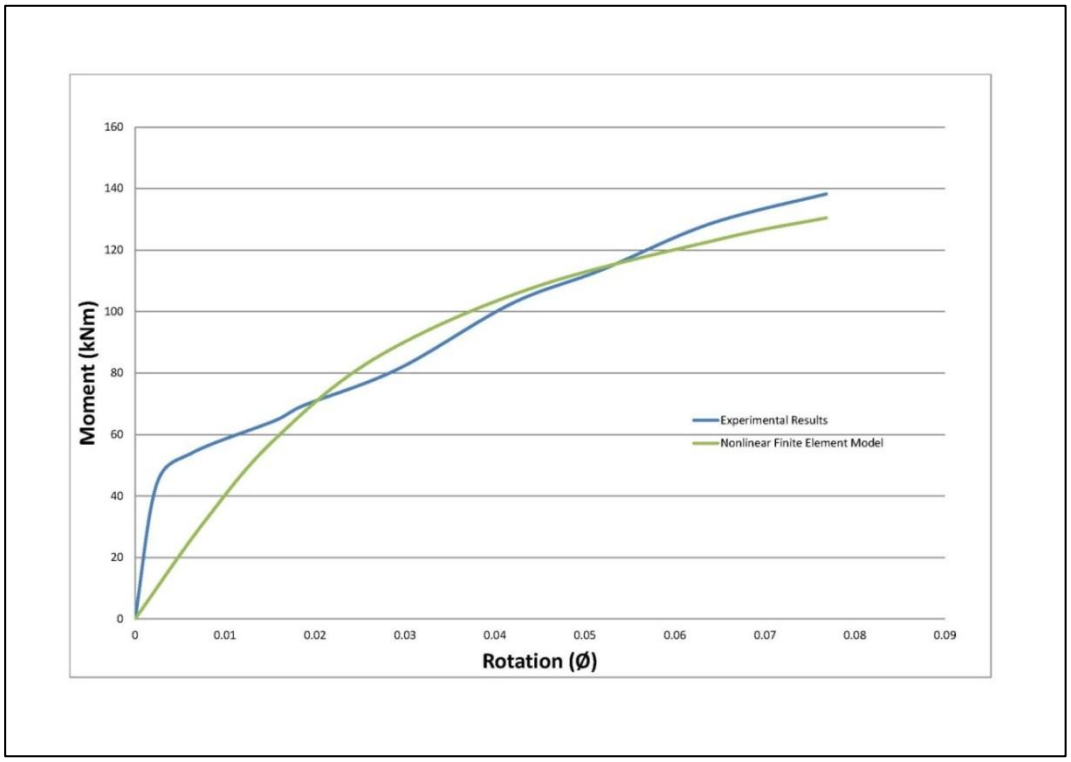

Figure 3.19 Comparison of Moment-Rotation Responses for BCC-10 Specimen of Calado et al. (2000)

In Figure 3.19, it is observed that the initial stiffness is overly underestimated once again, yet the final plastic moment capacity is closely captured when compared with experimental data. Undeformed and deformed shapes of the finite element models for BCC10 specimen could be found in Appendix A.

As a conclusion of these three specimens, initial stiffness values of all simulated specimens of Calado et al. (2000) are underestimated, while the final plastic moment capacities of the specimens are closely captured. In terms of deformation of the connection region, finite element simulations can closely capture the deformations at the ultimate loading point, yet the flexibility of the connection region under much lower deformations are in great error when compared with experimental measurements. This discrepancy occurs despite the fact that same modeling approach as done in Azizinamini's specimens was followed for Calado et al. (2000) with the fact that the documented pretension value by Calado et al. (2000) was used on the bolts for consistency.

3.3 Komuro's Experiments

Komuro et al. (2003) published a conference paper on the monotonic and cyclic behavior of semi-rigid connections. As part of their study, they have considered three

different specimen configurations, where one of them was top and seat angles (TSA) connection and two of them were top and seat angles with double web angles (TSDWA) connection. Same specimen configurations tested monotonically were also tested cyclically in order to assess the influence of cyclic loading on moment-rotation response of connections.

3.3.1 Material Properties

Komuro et al. (2003) carried out coupon tests in order to document the material properties of the parts used in the test specimens. The results of the coupon tests are provided in Table 3.5, where the stress-strain relationships of the materials are given in Figure 3.20. SS400 grade steel was used for all steel profiles, and F10T grade steel was used for the bolts.

Table 3.5 Coupon Test Results of the Materials, Komuro et al. (2003)

Location of Material		Grade	Young's Modulus E (GPa)	Poisson's Ratio υ_s	Yield Stress f_y (Mpa)	Tensile Stress f_u (Mpa)	Elongation (%)
Beam	**Web**	SS400	210	0.3	385	481	37.1
	Flange		210		325	463	39.4
Top / Seat Angle			210		282	449	44.6
Web Angle			209		315	469	41.7
Bolt		F10T	212		1060	1098	19.7

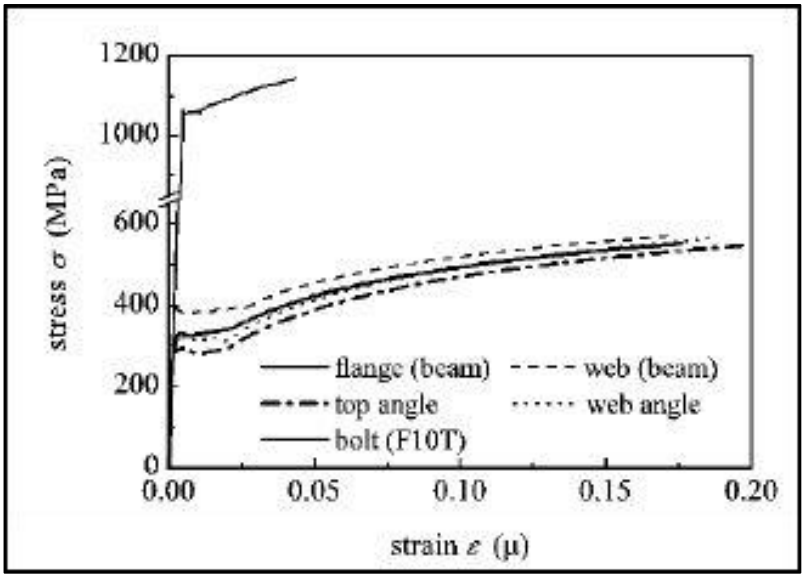

Figure 3.20 Stress – Strain Relationship of the Materials, Komuro et al. (2003)

3.3.2 Test Specimens

Within the scope of this thesis, all specimens tested by Komuro et al. (2003) are modeled by using ANSYS, and loaded monotonically for comparison. Geometric properties of the test specimens are provided in Table 3.6, and the test loading set up is given in Figure 3.21.

Table 3.6 Test Specimen Table of Komuro et al. (2003)

Specimen Number	Type of Test	Beam Section (mm)	Top & Bottom Flange Angles		Web Angles	
			Angle (mm)	Length (mm)	Angle (mm)	Length (mm)
W00	Static	H400 x 200 x 13 x 8	2 x L 150 x 100 x 12	200	-	-
W18	Static	H400 x 200 x 13 x 8	2 x L 150 x 100 x 12	200	2 x L 90 x 90 x 7	110
W29	Static	H400 x 200 x 13 x 8	2 x L 150 x 100 x 12	200	2 x L 90 x 90 x 7	220

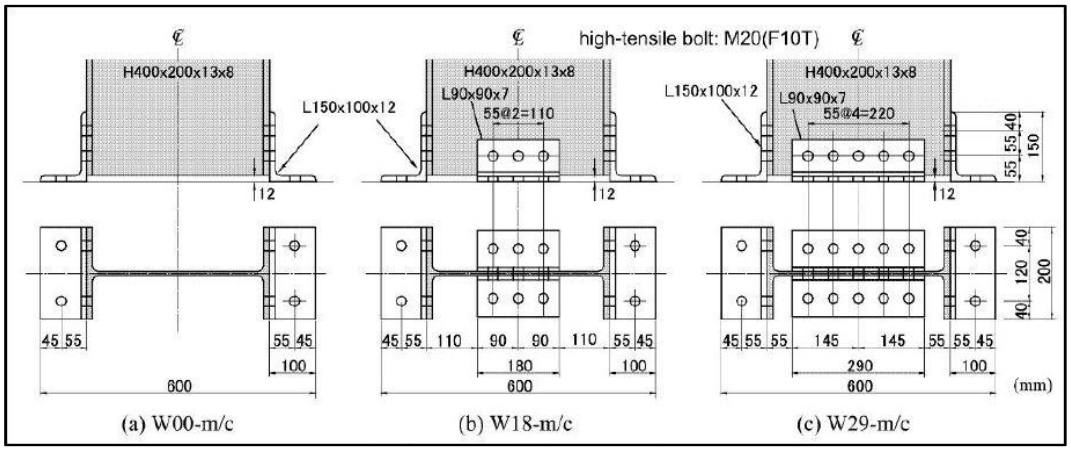

Figure 3.21 Experimental Test Setups, Komuro et al. (2003)

In all specimens, H400 × 200 × 13 × 8 type I profile beams were used and 12mm space between back profile plate and I profile beams was given by the researchers. Regarding to the study conducted in this thesis, it was observed that the space provided has great influence on moment-rotation results. For this reason, correct spacing between the beam profile and the base plate is used in the finite element models for consistency.

The top and seat angles specimen was named as W00 specimen by Komuro et al. (2003). The connecting angles were L 150 × 100 × 12mm in dimension, and 12 × M20 high

tensile F10T grade bolts were used for connecting the angles to other parts. W18 type of connection has the same connection materials and parts with W00 specimen and the following additional web angles and bolts were used: 2 × L 90 × 90 × 7 mm angles with 110mm length and 9 × M20 high tensile F10T grade bolts for connecting the web angels to other parts. For W29 specimen, larger web angles were used with 27 × M20 high tensile F10T grade bolts connecting the web angles to other parts. As a result, the moment capacity of W29 specimen was the greatest among all specimens.

The experimental test setup is presented in Figure 3.22, where the column of the test setup is fixed to the basement and the end of the beam is imposed a transverse displacement at its end. Instead of modeling the whole column assuming that it provides full restraint at end, only the top flange of the column is modeled in ANSYS, and the back face of the column's top flange is fixed. There was no data regarding the amount of pretension force applied on the bolts, thus similar to Calado et al. (2000)'s tests 88 kN pretension force is applied on all bolts.

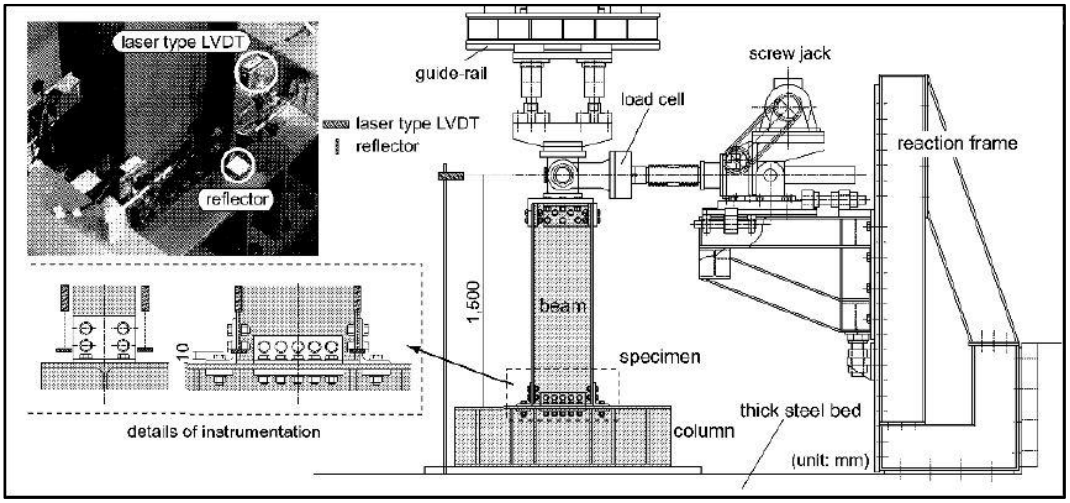

Figure 3.22 Experimental Setup of the Specimens, Komuro et al. (2003)

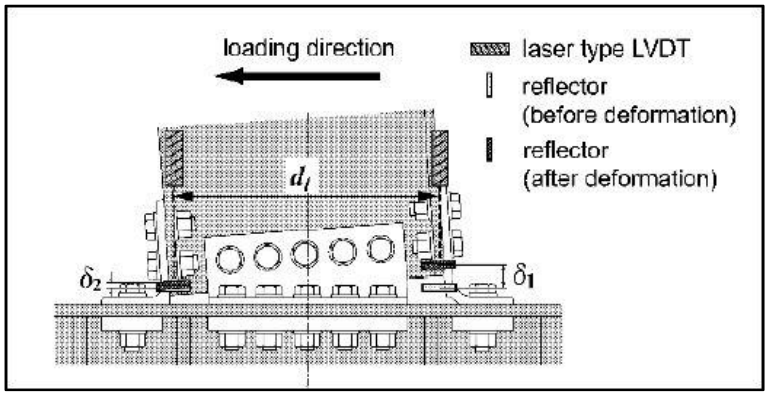

Figure 3.23 Deformed Shape of the Specimen, Komuro et al. (2003)

In terms of comparison of numerical and experimental results, first the pictorial representation of the deformed shape presented by Komuro et al. (2003) in Figure 3.21 can be compared with the deformed shape of the connection obtained from finite element simulation for W18 specimen in Figure 3.25. Evident from this comparison, the physical deformations in the connection region is accurately captured at the end of loading of the specimen.

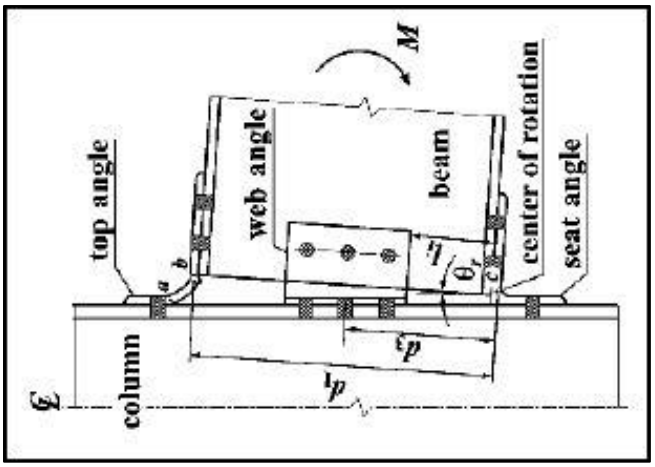

Figure 3.24 Deformed Shape, Komuro et al. (2003)

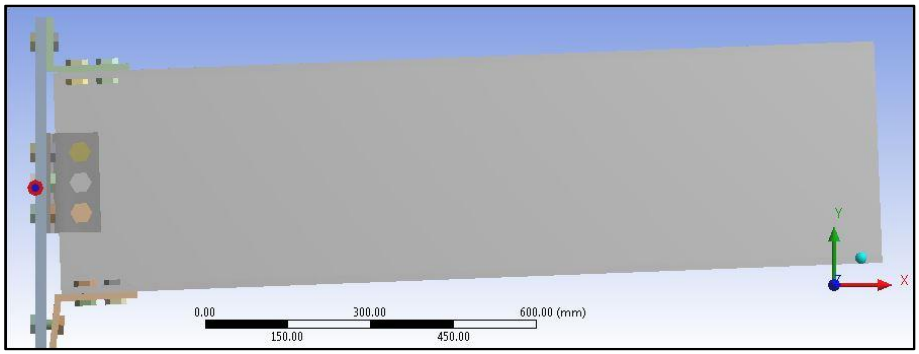

Figure 3.25 Deformed View of W18

For the comparison of moment-rotation responses, only the top and seat angles with double web angle specimens are considered. First W18 specimen is presented here, where the geometric properties are available in Table 3.6. In the finite element model, all bolts were first loaded with a pretension force of 88 kN. 24,448 nodes and 9,743 elements were used in order to model the nonlinear behavior of W18 specimen in ANSYS.

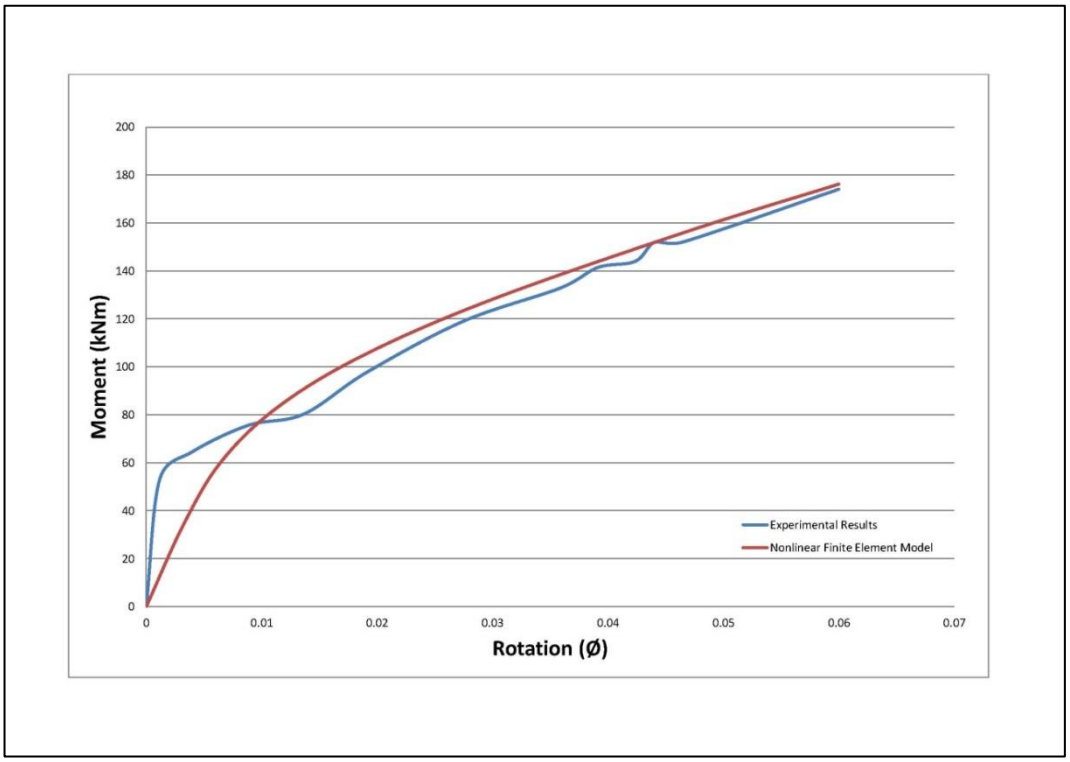

Figure 3.26 Comparison of Moment-Rotation Responses for W18 Specimen of Komuro et al. (2003)

Comparison of moment-rotation response obtained from numerical simulation reveals underestimated initial stiffness for the connection when compared with the experimental data in Figure 3.26. Despite this discrepancy, the plastic moment capacity of the connection is closely captured by the finite element model.

Last specimen compared from Komuro et al. (2003)'s tests is W29 specimen. In the finite element model, all bolts were first loaded with a pretension force of 88 kN once again, then the lateral loading was applied. 24,403 nodes and 9,581 elements were used in order to model the nonlinear behavior of W29 specimen in ANSYS.

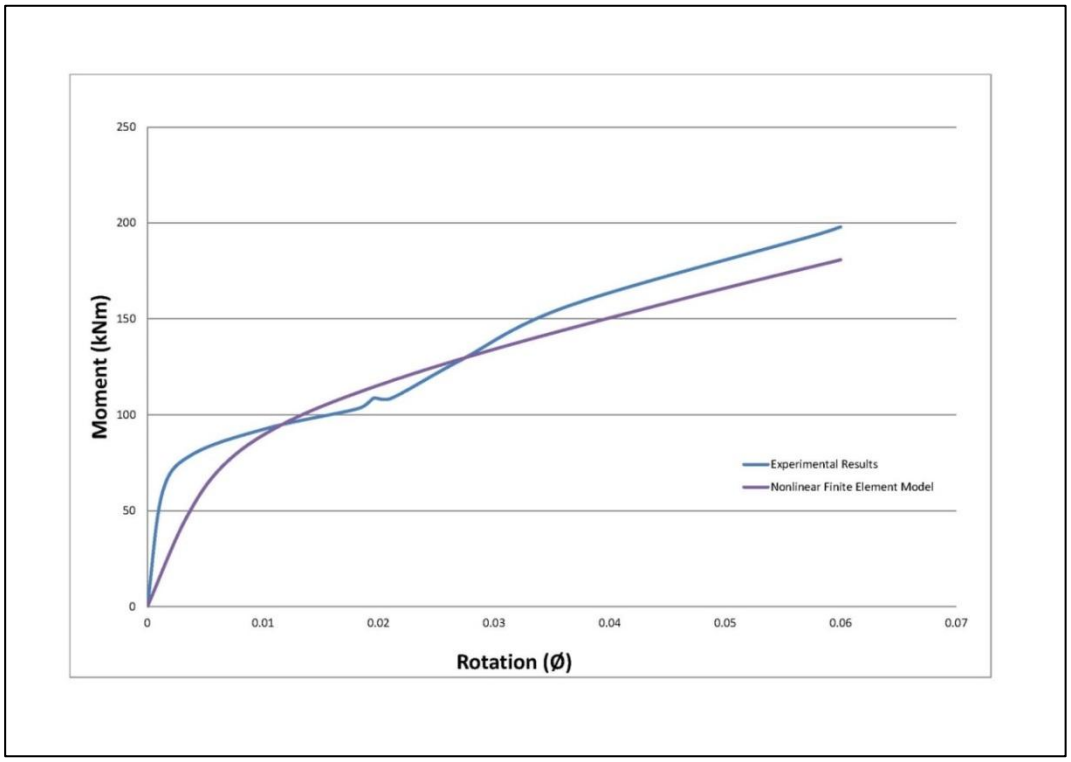

Figure 3.27 Comparison of Moment-Rotation Responses for W29 Specimen of Komuro et al. (2003)

Moment-rotation responses of the numerical and experimental results are given in Figure 3.27. It is observed that the overall moment-rotation curve from finite element simulation is close to the experimental one, but the initial stiffness is once again underestimated, and the plastic moment capacity is slightly underestimated, as well.

3.4 Remarks on Numerical Analysis

In any comparative study deviations exist between experimental data and numerical simulations. Uncertainties in experimental work stem from the experimental set up, measurements of geometrical and material data, imposition of loading and boundary conditions and lastly due to error in readings of experimental results. Assuming that all these are close to perfection in an experimental study, it is also possible to witness problems in the documentation of the conducted study, as well. On the other end, numerical studies may contain significant amounts of mistakes, as well. These are mainly caused by the person improperly modeling the problem at hand and insufficient knowledge and use of an available software package and its available modules. Lastly, it is also possible that a certain finite element package may not sufficiently replicate the real physical action due to lack of analysis modules in it.

The specimens modeled in this thesis were all top and seat angles with double web angles (TSADWA) connections. Most of the material and geometrical properties and test setup configuration were available in the specimens considered for analysis; however, the friction coefficient values were all missing in the experimental documentations, and properties on bolts and pretension values were missing in some of the tests. Furthermore, it was assumed that the column connecting to the connection provides full restrained and it would be sufficient to model only the top flange of the column.

CHAPTER 4

SUMMARY AND CONCLUSION

4.1 Summary

The first chapter of this thesis started with general introduction on semi-rigid steel connections and then the motivation of the thesis was presented and semi-rigid connection types and properties were given. Within the scope of this thesis, only top and seat angles with double web angles (TSADWA) connection type is considered, therefore Chapter 1 continued with the literature review on experimental studies and 3-D finite element simulations on TSADWA connection.

In the second chapter of this thesis, nonlinear finite element modeling of semi-rigid connection steps was defined in detail through the use of ANSYS Workbench FE program. Modeling capabilities of the program and material modeling module have been stated, and the meshing procedure of all parts of the connection is defined. Afterwards, the difficulties on setting up such complicated connection models in ANSYS were discussed with regards to the time consumption and robustness of simulations. Then, contact modeling module in ANSYS Workbench was presented through a demonstration example. At the end of the chapter, application of pretension force on a bolt was documented and an example was given.

In the third chapter, the nonlinear finite element modeling results and comparisons for previous experimental studies on TSADWA connection were presented. Totally 10 experimental studies was analyzed from 3 different researches, that are respectively; Azizinamini (1985), Calado et al. (2000) and finally Komuro et al. (2003). For each experimental specimen group, information was given with regards to the material, geometric properties and test setup. Then, the results obtained from finite element simulations were compared with the experimental data.

4.2 Conclusion

Researchers have been focusing on studying and assessing the nonlinear behavior of various types of semi-rigid connections in the last two decades. Experimental and numerical studies conducted on semi-rigid connections are few especially on top and seat angles with double web angles (TSADWA) connection. The first experiment conducted was in 1936, followed by 1985 study by Azizinamini. There is a rising interest on the study of the monotonic and cyclic behavior of this connection type in the last decade. This interest also

led some researchers to conduct numerical studies on this connection type; however, the numerical studies up to now did not try to compare all of the experiments conducted on this connection type. Due to scarce data, it can be concluded that there is still lack of knowledge on the physical actions going on especially through the cyclic loading of TSADWA connection. Conflicting conclusions with regards to the influence of cyclic loading on overall energy dissipation characteristics exist in the literature.

Within the scope of this thesis, it was intended to validate the results of all tests conducted on TSADWA connection specimens in literature. The purpose in this regards is to assess whether the current advanced finite element programs can provide means for such a simulation through detailed modeling of all nonlinearities occurring in the connection region. The results of moment-rotation curves obtained from finite element simulations were compared with experimental results. Initially, conducting cyclic analysis was targeted; however, this effort was quickly terminated due to difficulties in time consumption of analysis and furthermore the cyclic simulations did not provide satisfactory results when compared with experimental ones. It was later realized that no one in literature presented cyclic numerical results on bolted steel connections by using 3-D finite element software and considering contact, friction, material and geometric nonlinearities; thus this clearly points out a common problem faced in the scientific community. For this reason, the thesis focused on only comparison of monotonic responses of the selected specimen groups that are not all together modeled in a numerical simulation before.

The comparison studies and discussions resulting from the detailed finite element models conducted within the scope of this thesis provide a comprehension for future structural engineers on bolted semi-rigid steel connections, especially TSADWA connection type.

The main conclusions of this thesis are listed below:

- Use of ANSYS finite element program gives physically accurate representations of the deformed shape of the connection region when compared with experimental ones.
- The initial stiffness of the moment – rotation curves obtained from finite element simulations yielded lower estimates compared with the experimental ones.
- Plastic moment capacities of the connection specimens have been closely captured through numerical simulations.
- Cyclic modeling studies were implemented in the beginning of the thesis. Due to enormous time consumption and convergence problems, conducting cyclic analysis on bolted semi-rigid connections had been terminated. Furthermore, the cyclic moment-rotation curves obtained from cyclic analysis did not provide close estimations with the experimental ones.
- To the knowledge of author of this thesis, there is no documented study on the cyclic simulation of bolted semi-rigid connections in literature. This clearly indicates a common problem faced in the scientific community. Despite all technological improvements, the current state of advanced finite element programs cannot satisfactorily provide sufficient means to conduct cyclic analysis on such type of connections.

- Despite the fact that technological improvements in computers and numerical methods are immense, conducting even monotonic analysis on such complicated 3-D models require significant amount of expertise and careful modeling of the problem. A researcher/engineer should always be aware of the fact that a software package may not contain all necessary means to successfully carry out an intended numerical simulation, especially when verification with experimental data is sought.
- Documentations on experiments conducted on TSADWA connection are not complete enough to provide all parameters needed to conduct a numerical verification study.

4.3 Recommendations for Future Researchers

The following recommendations are listed as a result of the problems encountered during finite element modeling and analysis of bolted semi-rigid connections conducted in this thesis:

- Due to lack of cluster computers, cyclic analysis was not carried out as part of this thesis. Future researchers should definitely use the parallel processing capabilities with advanced finite element programs in order to assess the state of modules and libraries provided by software packages.
- Current thesis study considered using only ANSYS for numerical simulations. In order to assess the state of current finite element packages, ABAQUS and MSC-Nastran should also be taken into account.
- It would be helpful to conduct simple experimental tests, such as the numerical demonstrations considered in Chapter 2. By conducting these experiments in the laboratory, numerical verification studies can be conducted on much smaller scale specimens than the complicated TSADWA connection configurations. In this regards, ANSYS and ABAQUS may be used at least to assess the strengths and weaknesses of each software package to simulate nonlinear contact, friction and application of pretension force.

REFERENCES

ANSYS Workbench Finite Element Analysis Program, V.12.1.0 ANSYS Inc. 2

ANSYS Workbench User Manual V.12.1.0 ANSYS Inc.

Azizinamini, A. (1985). “Cyclic characteristics of bolted semi-rigid steel beam to column connections” PhD thesis, University of South Carolina, Columbia

Calado, L., G. De Matteis and R. Landolfo (2000). "Experimental response of top and seat angle semi-rigid steel frame connections." Materials and Structures 33(8): 499-510

Chen, W.-F., N. Kishi and M. Komuro (2011). Semi-rigid connections handbook, J. Ross Publishing.

Citipitioglu, A., R. Haj-Ali and D. White (2002). "Refined 3D finite element modeling of partially-restrained connections including slip." Journal of Constructional Steel Research 58(5): 995-1013

Danesh, F., A. Pirmoz and A. S. Daryan (2007). "Effect of shear force on the initial stiffness of top and seat angle connections with double web angles." Journal of Constructional Steel Research 63(9): 1208-1218

Kishi, N. and W.-F. Chen (1990). "Moment-rotation relations of semirigid connections with angles." Journal of Structural Engineering 116(7): 1813-1834

Komuro, M., N. Kishi and R. Hasan (2003). Quasi-static loading tests on moment-rotation behavior of top-and seat-angle connections. STESSA Conference

Krishnamurthy, N. (1980). "Modelling and prediction of steel bolted connection behavior." Computers & Structures 11(1): 75-82

Krishnamurthy, N. and D. E. Graddy (1976). "Correlation between 2-and 3-dimensional finite element analysis of steel bolted end-plate connections." Computers & Structures 6(4): 381-389

Rathbun, J. Charles (1936), "Elastic Properties of Riveted Connections", Transactions of the American Society of Civil Engineers, Vol. 101, pp 524-563, 1936

The AISC Specification for Structural Steel Buildings (2005)

Uslu, C.H. and A. Saritas (2010). "Mathematical Models for Semi-Rigid Connections: Top and Seat Angle with Double Web Angles Connection" 9th International Congress on Advances in Civil Engineering, Turkey

Yang, J.-G., T. Murray and R. Plaut (2000). "Three-dimensional finite element analysis of double angle connections under tension and shear." Journal of Constructional Steel Research 54(2): 227-244

APPENDIX A

NONLINEAR FINITE ELEMENT MODEL SETUPS FOR AZIZINAMINI (1985)

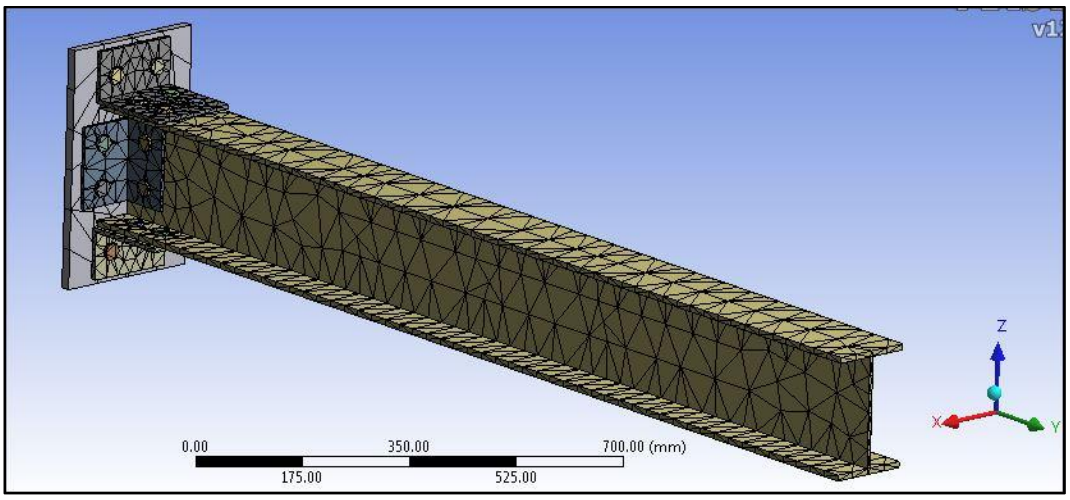

Figure A. 1 Azizinamini 8S1 Undeformed

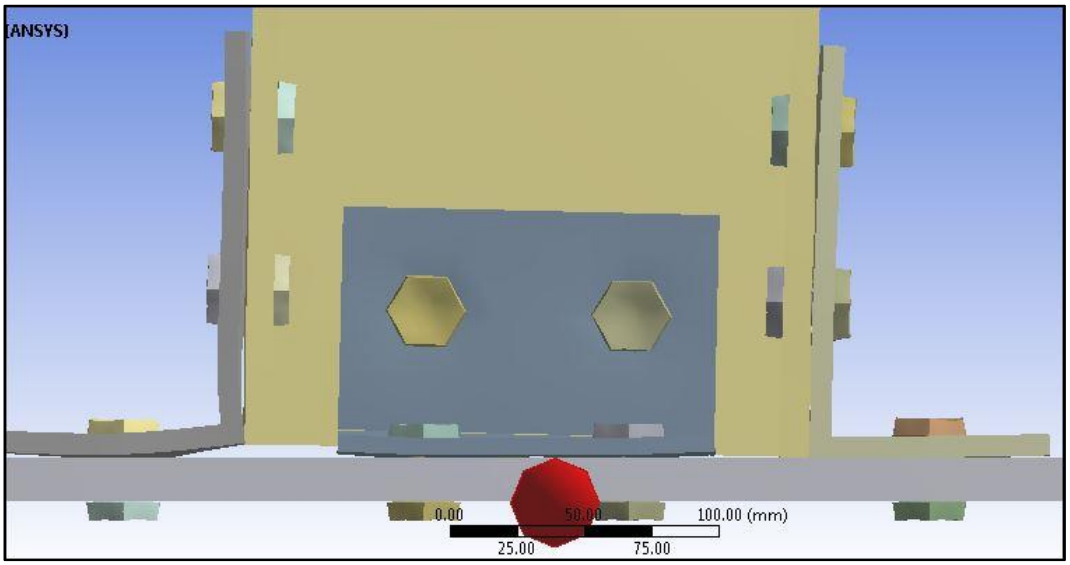

Figure A. 2 Azizinamini 8S1 Deformed

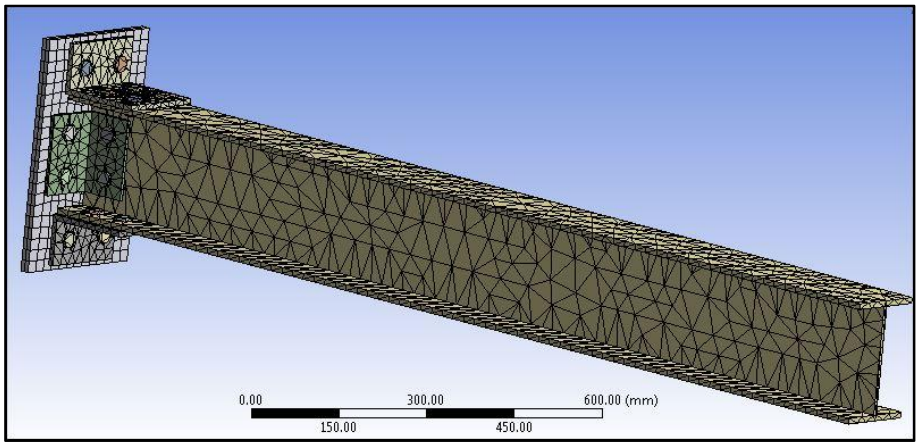

Figure A. 3 Azizinamini 8S2 Undeformed

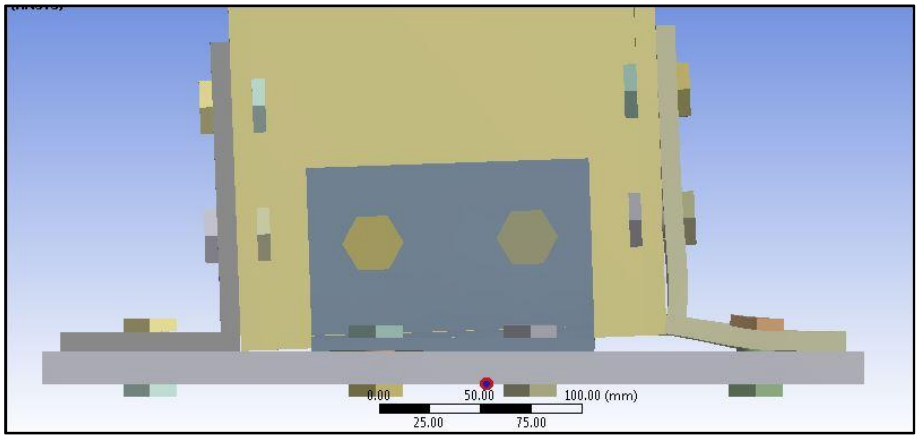

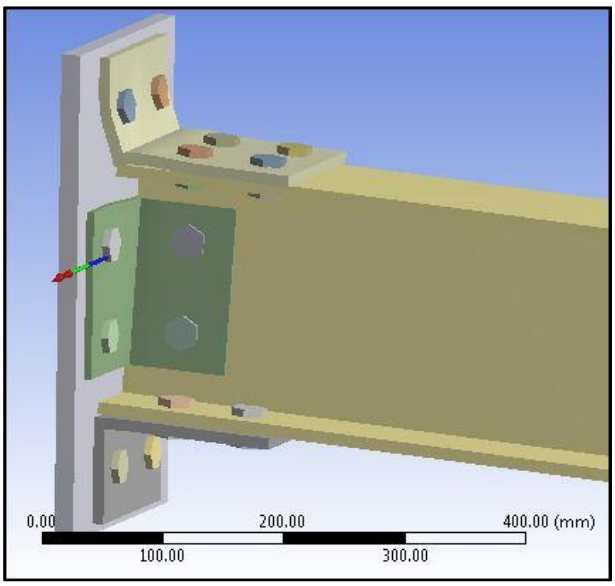

Figure A. 4 Azizinamini 8S2 Deformed Shapes

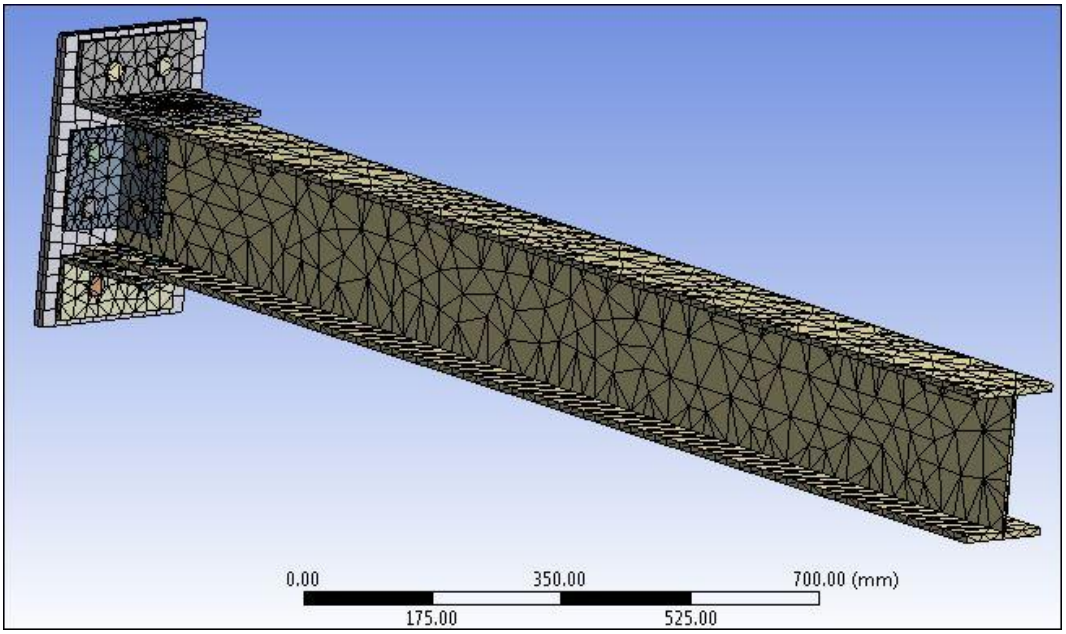

Figure A. 5 Azizinamini 8S3 Undeformed

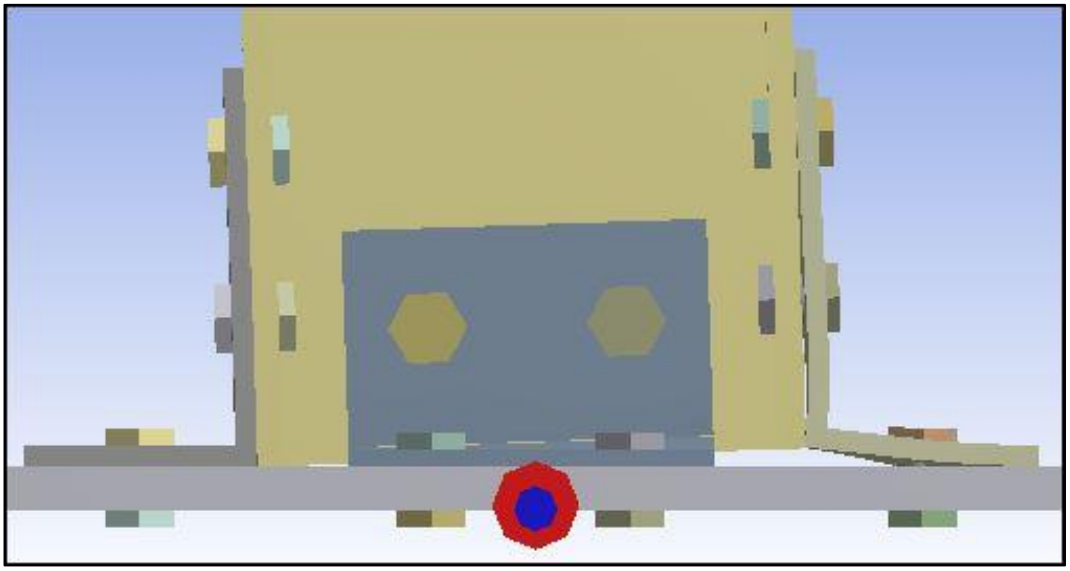

Figure A. 6 Azizinamini 8S3 Deformed

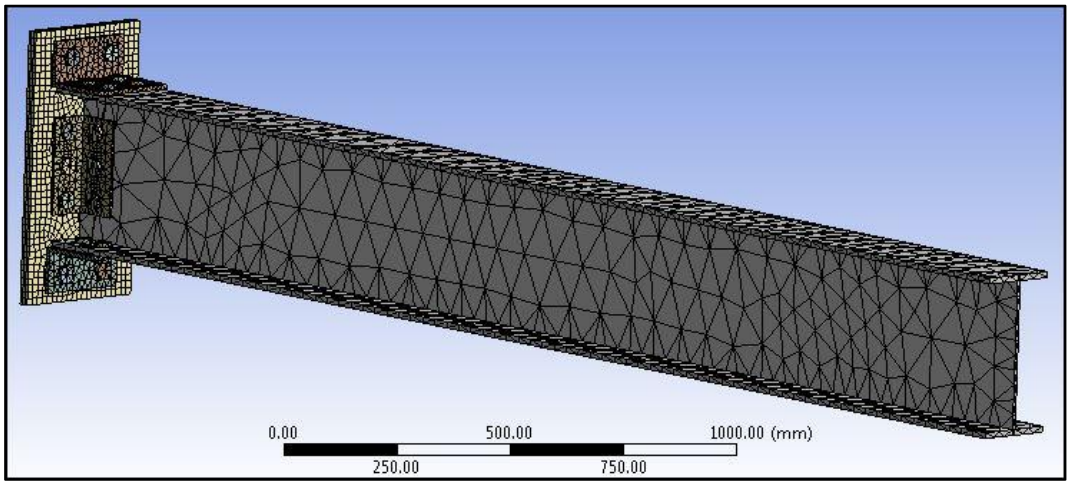

Figure A. 7 Azizinamini 14S1 Undeformed

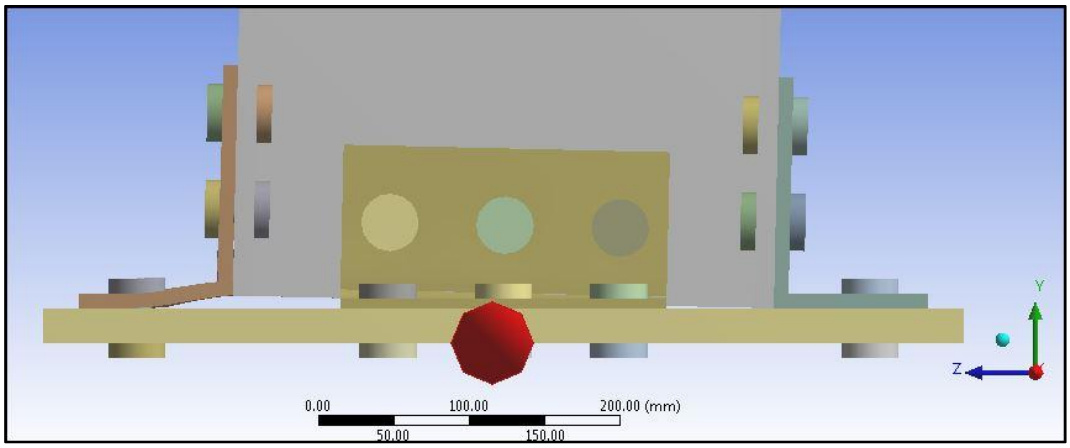

Figure A. 8 Azizinamini 14S1 Deformed

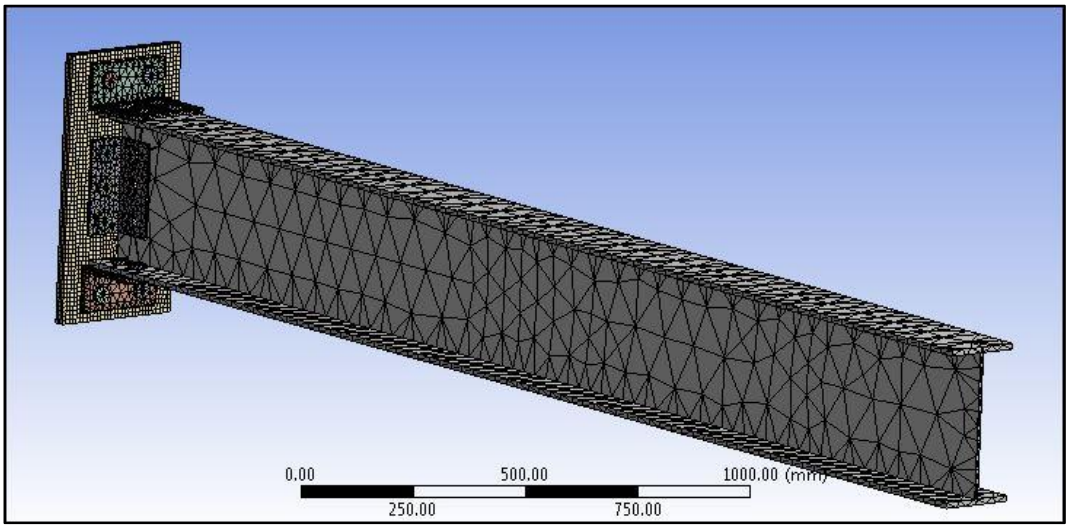

Figure A. 9 Azizinamini 14S5 Undeformed

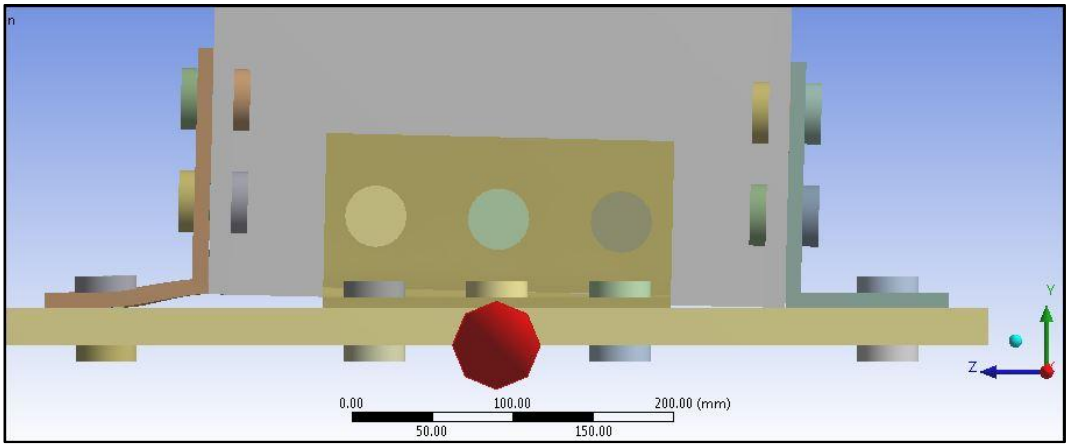

Figure A. 10 Azizinamini 14S5 Deformed

NONLINEAR FINITE ELEMENT MODEL SETUPS FOR CALADO ET AL. (2000)

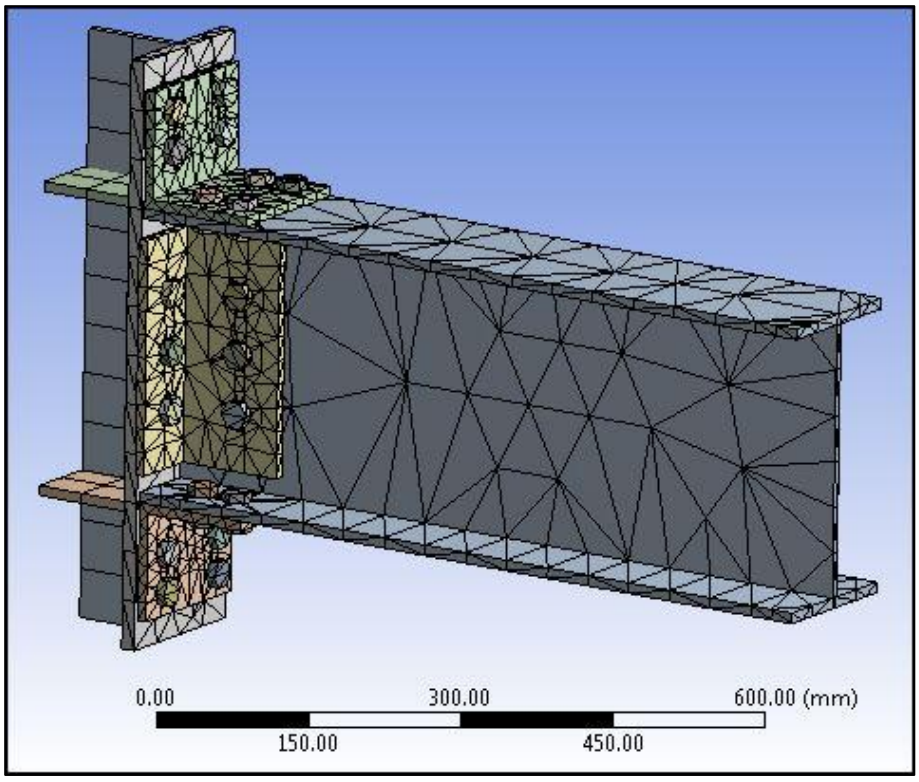

Figure A. 11 Calado BCC-7 Undeformed

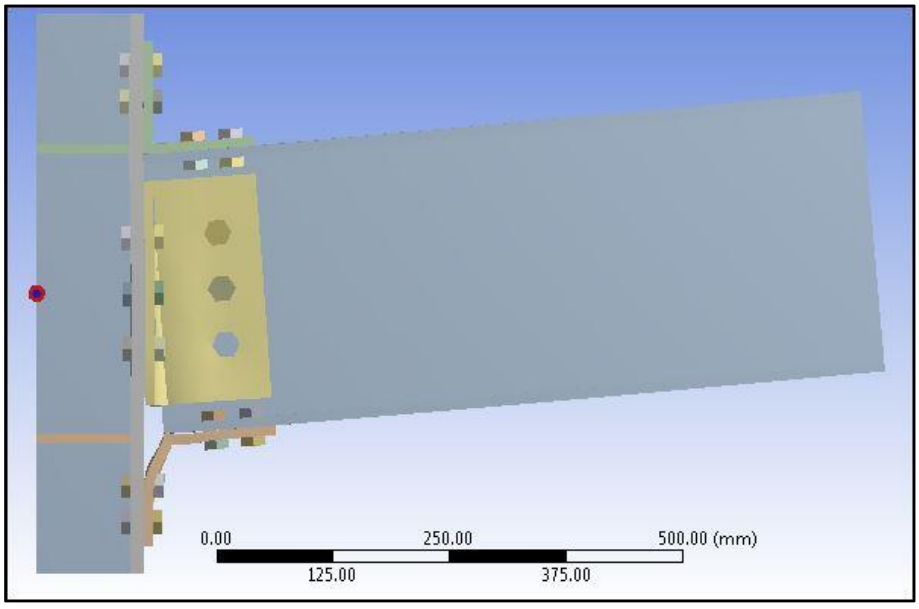

Figure A. 12 Calado BCC-7 Deformed

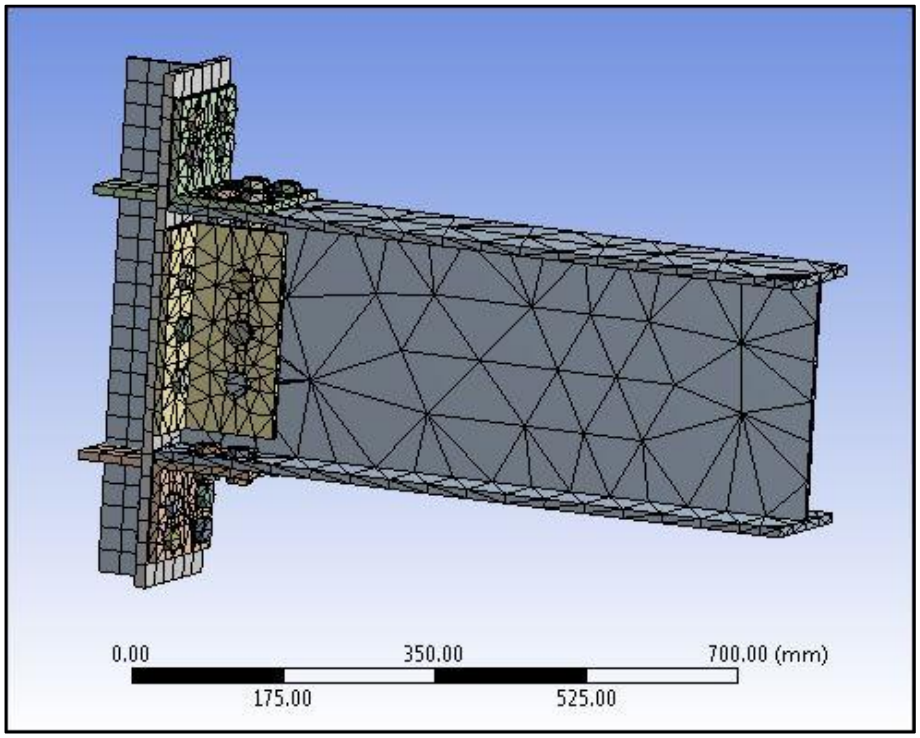

Figure A. 13 Calado BCC-9 Undeformed

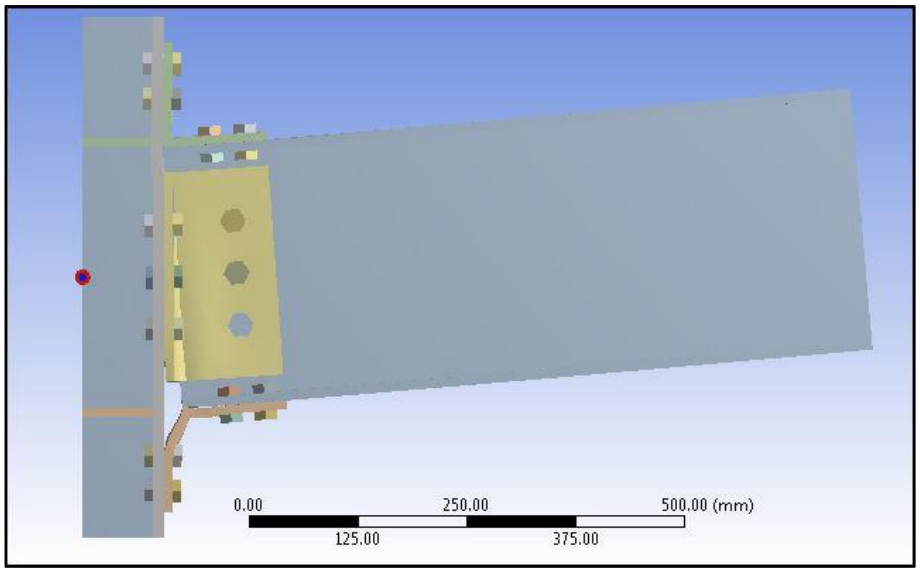

Figure A. 14 Calado BCC-9 Deformed

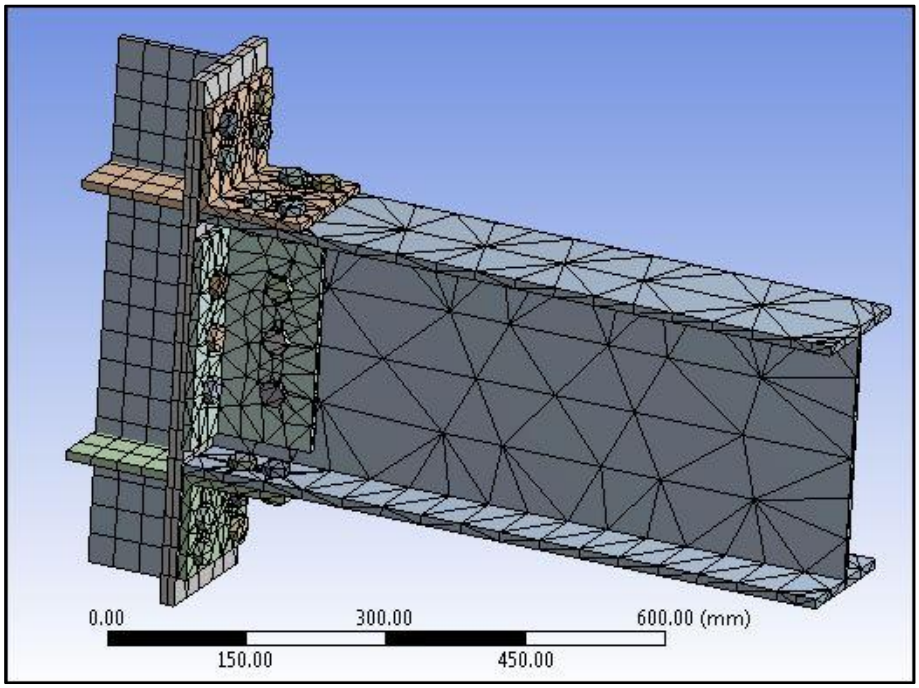

Figure A. 15 Calado BCC-10 Undeformed

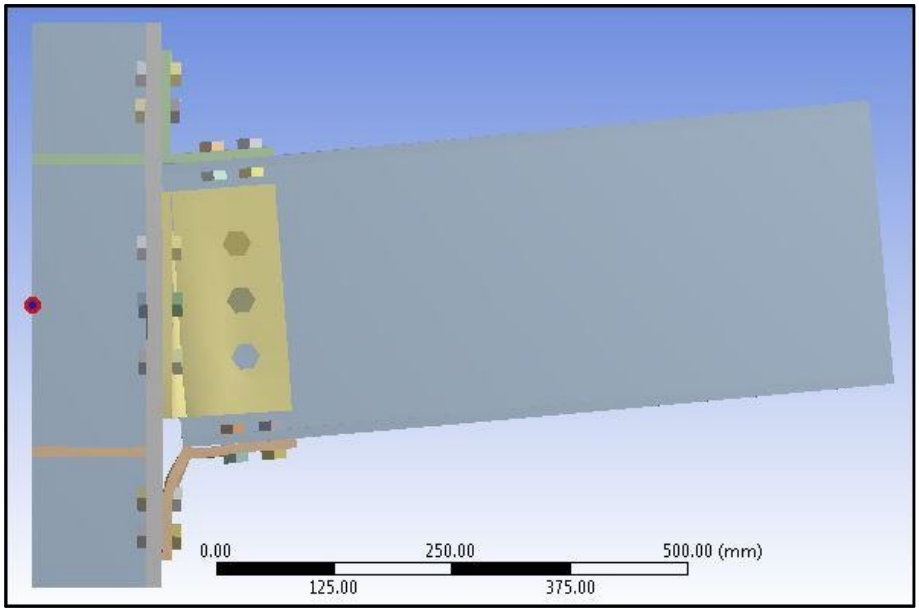

Figure A. 16 Calado BCC-10 Deformed

NONLINEAR FINITE ELEMENT MODEL SETUPS FOR KOMURO ET AL. (2003)

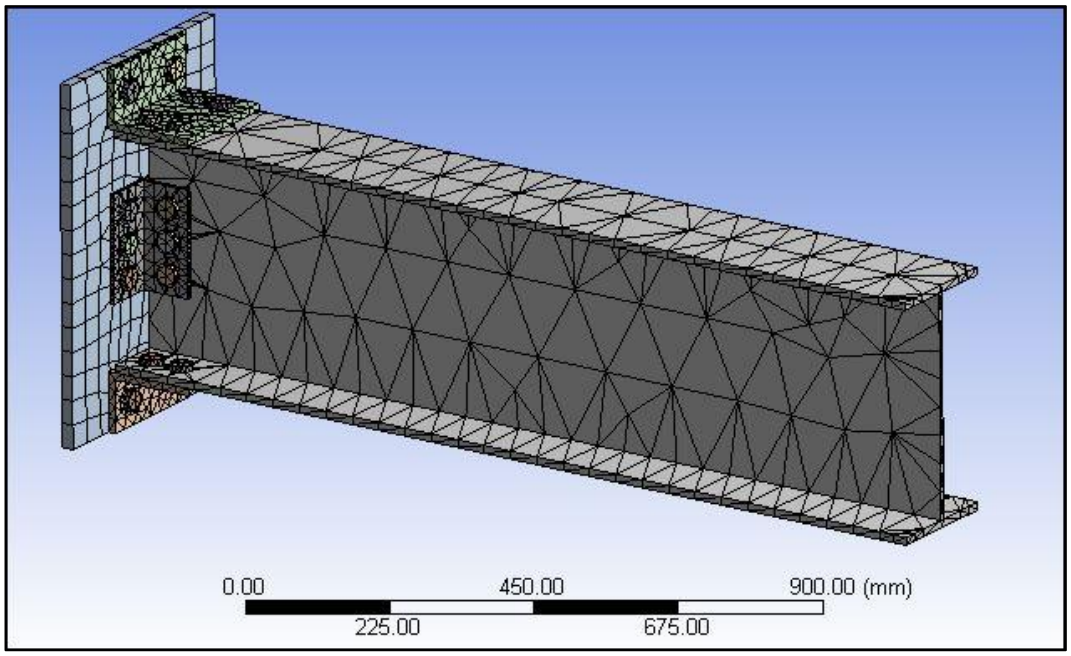

Figure A. 17 Komuro W18 Undeformed

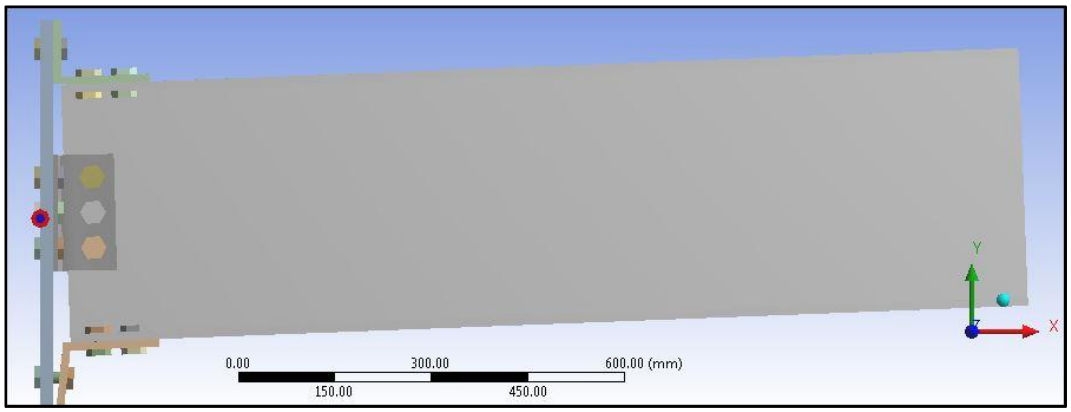

Figure A. 18 Komuro W18 Deformed

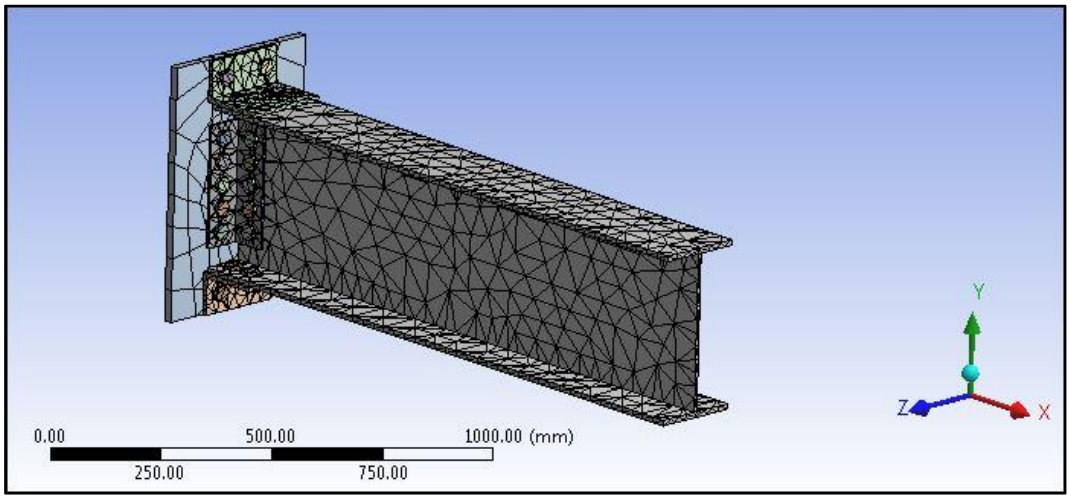

Figure A. 19 Komuro W29 Undeformed

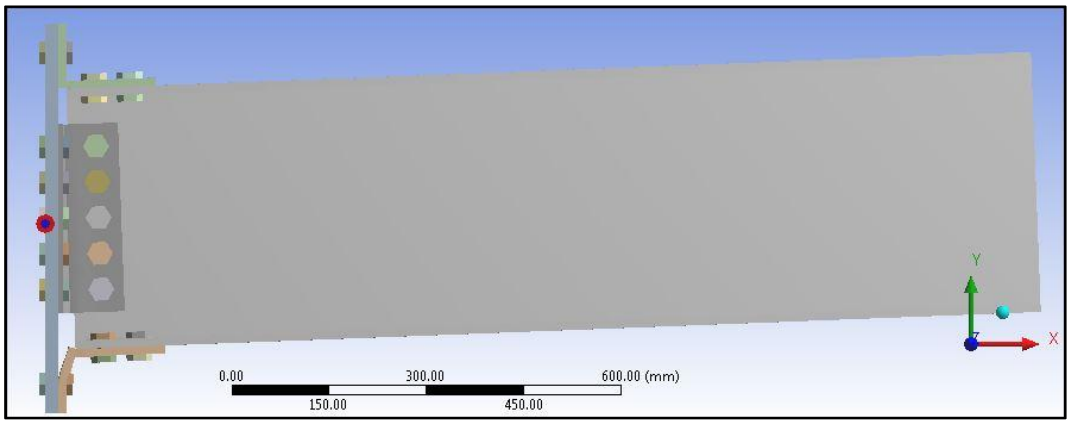

Figure A. 20 Komuro W29 Deformed